Development and Calibration of a Model for Tracking Dispersion of Waters from Narragansett Bay Commission Facilities within the Providence River & Narragansett Bay

Final Report to
The Narragansett Bay Commission
June 2007

Prepared by
Deanna Bergondo and Chris Kincaid

Graduate School of Oceanography
University of Rhode Island
Narragansett, RI 02882

1.0 Introduction

Episodic summer hypoxic events are of growing concern for the upper parts of Narragansett Bay, the Providence River and Greenwich Bay. In effort to better understand the processes surrounding these events, a series of buoys have been deployed throughout the bay equipped with sensors to measure important physical and chemical properties including, temperature, salinity, dissolved oxygen, pH and chlorophyll. Monthly surveys of temperature, salinity and oxygen in the Upper Bay have also been conducted during the summer months. In addition, the Narragansett Bay Commission funded an observational program (2001-2002) headed by Microinorganics to characterize spatial variability in circulation and chemical transport within the Providence and Seekonk Rivers during each seasonal period. The data set on currents collected by Kincaid's group with Narragansett Bay Commission funding provides the most detailed spatial images on circulation ever collected for Narragansett Bay.

One of the most striking features of the Narragansett Bay Commission ADCP data surveys is the identification of dominant outflow regions of the Providence River where flushing is expected to be very efficient. In addition, the surveys identified key stagnation regions, where waters are expected to remain unmixed over multiple tidal cycles thereby greatly increasing residence times. The vast majority of estimates for residence time in estuarine systems are based on the assumption of complete mixing. These data suggest the Providence River does not behave in this way, suggesting previous flushing estimates may be inaccurate. These diverse data sets provide clues as to the relative importance of different environmental factors, including tidal range, wind speed, direction and duration, and fresh water input, on the occurrence of hypoxia in Narragansett Bay. However, each data set does not provide both the spatial and temporal scales necessary to fully resolve the system.

The purpose of this study is to use a combination of numerical modeling and new observational data to better calibrate transport models and provide more accurate estimates on flushing rates for Narragansett Bay Commission releases entering the Providence River, either from Fields Point or the Seekonk River. We have conducted a detailed hydrographic survey within the Providence River, which included four months of bottom mounted Acoustic

Doppler Current Profiler (ADCP) data from three locations and a 12 hour tidal survey of the currents along three transects of the Providence River (Figure 1). In addition, we have generated high resolution grids of the Providence and Seekonk Rivers for the Regional Ocean Modeling System (ROMS) to use to examine the influence of winds, tides and river flow on regional flushing rates.

2.0 Data Collection

RD Instruments Broadband Acoustic Doppler Current Profilers (ADCP) were used in this study to measure water column currents. The ADCP consists of an array of four transducers oriented such that sound beams are transmitted out 90° angles from each other and a known angle from the central axis of the instrument. Sound pulses emitted by the transducers are reflected by particles throughout the water column, such as biological and other particulate matter. The reflected sound pulses are Doppler shifted due to the movement of the particles in the moving water. The ADCP processes the Doppler shifted return echoes to obtain along-beam velocity components which are then combined for each transducer and converted into a three-dimensional (3-D) velocity pattern. Through a process called "range gating" the ADCP listens to the returning sound pulses over uniform time increments. Progressively later time increments correspond to energy returning from greater depths. In this way velocities are resolved into depth cells, or bins. For each energy pulse sent out, or set of energy pulses, which are subsequently averaged, the resulting velocity versus depth profile is called an "ensemble".

2.1 Bottom Mounted ADCPs

Four bottom mounted instruments were deployed in the Providence River from June through October 2006 (Figure 1, Table 1). A 1200 kHz ADCP was deployed at the mouth of the Seekonk River in approximately 6 m of water. A 300 kHz ADCP was deployed in the middle of the channel in the West Passage near the northern tip of Prudence Island in approximately 15 m of water. A 600 kHz ADCP was deployed in the middle of the channel in the East Passage near the northern tip of Prudence Island in approximately 14 m of water. A 1200 kHz ADCP was deployed on the shallow western side of the East Passage near the north tip of Prudence Island in approximately 6 m of water. Data were collect at 10 minute intervals with 120 pings per ensemble. The bottom mounts were deployed from the NBC boat, a 25' Parker. Pick-up lines of 1.5 times the water depths were dropped along channel for retrieval by grappling for the Seekonk and East Passage Channel mounts. The West Passage and East Passage shallow mounts were equipped with acoustic releases for recovery. Notus pingers were attached to all of the mounts.

The observed magnitude and direction of the currents was used to determine the flow along and across the channel. Data gaps less than one hour in length were filled using a linear regression. Residual velocity components were calculated by running a 5^{th} order low pass Butterworth filter to remove frequencies higher than 33 hours. Values for wind speed and direction were obtained from the National Climate Data Center (NCDC) for the T.F. Green station in Warwick, RI. Daily mean values of freshwater discharge in cubic feet per second were obtained for the Blackstone River from the United States Geological Survey stream gauge in Massachusetts.

2.2 Boat Mounted ADCPs

For the boat mounted work, a 600 kHz broadband ADCP instrument was mounted to the side of the NBC 25' Parker. Data were collected by driving along lines, called "transects" (Figure 1). Energy pulses were sent out on average every 5 seconds. Given an average boat speed of 1 m/s, a velocity ensemble is collected roughly every 5 meters. Therefore, over a complete transect information is obtained on 3-D velocity as a function of both depth and horizontal position. Plots can be made showing velocity contours through a vertical slice of the river oriented along the transect line.

The goal of the hydrographic surveys was to characterize flow patterns between the East and West Passages. The transect consisted of two lines across the northern tip of Prudence Island (Figure 1), one along the West Passage and one along the East Passage. The ADCP data was collected using standard water mode of 4, with depth bins of 50 cm. A SeaBird SB19 CTD was dragged behind the boat at roughly 1 meter depth for all transects.

Sampling began on July 11, 2006 at 6:47 am GMT, on the western side of the West Passage then another transect was done across the East Passage. The first set of transects coincided with the low tide while the forth and fifth sets of transects centered on the high tide. A summary of the data collection locations and times is given in Table 2.

2.3 Numerical model

2.3.1 Providence River Model

The numerical model ROMS (Regional Ocean Modeling System) (Shchepetkin and McWilliams, 1998; 2003; 2005) version 2.2 was applied to the Providence River with horizontal grid resolution of less than 150 meters (Figure 1). A ten second time step was used for the model. The bathymetry data was obtained from the National Geophysical Data Center 3-arc-second Coastal Relief Model and was smoothed with a single pass of a Shapiro filter. The kappa-epsilon parameterization was used for the generic length scale (GLS) turbulent closure scheme. This scheme was chosen based on model runs conducted in April 2005 comparing various GLS parameterizations for the Providence River. The open southern boundary was located just north of Prudence Island. Sea-level height and velocity were defined at the southern open boundary based on seven harmonics (M_2, N_2, S_2, K_2, O_1, M_4, M_6) determined from an ADCIRC simulation of the western Atlantic (Luettich et al., 1992). Multiple inputs for point sources were incorporated to represent the Blackstone/Seekonk, Pawtuxet, Woonasquatucket, and Moshassuck rivers, as well as the Fields Point WWTF discharges. ROMS incorporates the air-sea flux parameterizations (momentum, sensible heat, and latent heat) which allowed for simulation of surface heating/cooling (thermal stratification) in the Providence River. The 2005 ADCP and YSI data have been used to calibrate the Providence River model.

2.3.2 Seekonk River Model

The Regional Ocean Model (ROMS) version 2.2 was configured for the Providence and Seekonk Rivers with a focus on modeling processes within the Seekonk River. The boundaries of the grid extend in longitude from 71.41° W to 71.30° W and from 41.71° to 41.88° N in latitude. Figure 2 shows the extent of the Seekonk model grid in map view, running from the mouth which coincides with the mouth of the Providence River to the head of the modeled estuary near a constriction point directly south the I-95 bridge.

The model grid consists of 240000 nodes with 400 nodes in the east-west direction (x) and 600 nodes in the north-south (y) direction. Each computational element has uniform spacing in the horizontal (x-y) orientation at a grid resolution of 35m x 35m. The computational grid is three-dimensional (3-D) such that each grid element also has a vertical dimension (z). Vertical resolution varies spatially because the ROMS model uses a constant number of depth bins which are distributed throughout the water column. In this case we utilize ten vertical bins such that element (grid) resolution in z varies between .2 m and 1.8 m, depending on water depth. Bathymetry and coastline information was obtained from the National Geophysical Data Center (NGDC) at a 3 arc-second resolution.

The ROMS model requires data at the boundaries for forcing the simulations and data within the model domain for constraining model results. Environmental forcing includes tidal forcing, winds, runoff and salinity/temperature conditions of water at the head and mouth of the estuary. ROMS has been developed for grids that include the upper half of Narragansett Bay (the Providence River model reported above) and the full extent of Narragansett Bay including the inner shelf region of Rhode Island Sound. Tidal forcing for each of these models utilizes output from a large-scale circulation model called ADCIRC that covers the Eastern US coast/shelf (Luettich et al., 1992). Tidal constituents from ADCIRC were used to force tidal currents along our southern, open boundary. Significant effort was put into refining the magnitude of coefficients for the different tidal constituents to produce better fits between current meter data and modeled tidal flow (discussed below). The Seekonk current meter (ADCP) data set is discussed above. Discharge data for the Blackstone River was obtained from USGS for summer 2006. Discharge for the Tenmile River was not available through USGS, but a ratio of drainage areas of the two watersheds was used to interpolate daily values for the same time period (http://waterdata.usgs.gov/nwis/rt).

3.0 Results

3.1 Bottom Mounted ADCPs

Analysis of the bottom mounted ADCP data shows that the current velocities vary greatly between the four sites. The largest velocities are found in the Seekonk River where surface and bottom velocities are between ±1000 mm/s (Figure 3). The West Passage channel surface and bottom velocities are between ±500 mm/s (Figure 4). The East Passage channel instantaneous flows range between ±300 mm/s (Figure 5). The East Passage shallows has the lowest velocities, ±150 mm/s (Figure 6).

The tidally average velocities show interesting trends in the currents among the four stations. In the Seekonk River, the tidally average velocities are out at the surface and in at depth (Figure 3). The strength of the surface outflow appears to depend on the Blackstone River flow. In the West Passage, the residual flow is dependant on the winds, where a wind towards the north-eastward (winds from 120° to 300°) forces surface water into the upper bay and bottom water outward (Figure 4). The depth averaged residual flow shows a very small out flow at this location in the West Passage (< 50 mm/s). The residual flow in the East Passage channel indicates that the surface velocities are variable while the bottom and depth averaged flows are consistently inward (Figure 5). In the East Passage shallows, the surface flow is generally outward and the bottom flow inward (Figure 6). The depth averaged velocity is also outward. Periods when the depth averaged flow is inward, appear to be related to strong wind events from the south. The overall patterns in the residual flow in the East versus West Passage suggests inward flow in the deep channel of the East Passage and outward flow along the western shallows of the East Passage and in the channel of the West Passage. The observed counter-clockwise flow is consistent with our previous understanding of circulation in the Upper Bay.

3.2 Boat Mounted ADCPs

The twelve hour boat mounted ADCP survey from July 11, 2006 captured all stages of the tide at the two transect lines (Figure 1). Figure 7 shows the variability in discharge patterns between the East and West Passages. The tidal wave acts as a standing wave in both the East and West Passage. Both passages experience maximum positive discharge between low and high tide and maximum negative discharge between high and low tide. However, the West Passage experiences a double flood during the flood stage of the tide, the discharge drops slightly before reaching its maximum flood discharge (Figure 7). The double flood is most likely due to the influence of bottom friction and channel topography, or over tides, on the tidal wave.

The West Passage transects shows two-layer flow which is opposite of estuarine flow (Figure 8). During the ebb tide, the maximum outgoing currents are observed in the lower section of the channel. While during the flood tides the maximum currents are observed at the surface. This is likely controlled by an East Passage to West Passage pressure gradient. An interesting feature is observed on the western side of the channel, during the flood tide when flow is expected to be in, very low outward flows were present. The flow at this location is also outgoing on the ebb, so on average there is a strong outflow at this location.

The East Passage transects show a clear two layer flow across the channel (Figure 9). During the ebb tide, the outgoing currents are observed in the surface water, while water below 4.5m continues to flow inward. During the flood tides the maximum currents are at depths below 4.5 m.

3.3 Numerical model

3.3.1 Providence River Model

Model-data comparisons were made between the output of Providence River model and the available 2005 data. The model was run for a 30 day period representing conditions from July 2005. The horizontal and vertical mixing coefficients, wind, tide and river flow conditions were varied and the model output was compared to the YSI data from North Prudence and Phillipsdale and current data from the Providence River Shallow and Channel ADCPs (Table 3). The southern open boundary condition was also varied for the tracers. Runs NBC0705.016-030 were run with a radiation southern boundary with constant salinity values, runs NBC0705.031-034 were run with a nudging condition with salinity values obtained from the North Prudence and Popasquash buoys and runs NBC0705.035-036 were run with a clamped condition with salinity conditions obtained from the North Prudence and Popasquash buoys. Figure 10 shows the model-data comparison for salinity at Phillisdale under 1.5 times the river flow (model run NBC-0705.021). Based on visual inspection, the model captures the surface to bottom salinity gradient observed in the data.

Changing the southern open boundary condition for the tracer from radiation (NBC0705.024) to clamped (NBC0705.035) greatly improved the model results. Figure 11 shows the surface and bottom salt concentrations for the model compared to the North Prudence Buoy for both conditions. The model is better able to match the observed data when the clamped condition was used.

Figure 12 shows the daily values of surface and bottom salt concentrations for the clamped model (NBC0705.035) compared to the North Prudence Buoy. The model is able to capture the increases and decrease in stratification during this time. The linear regression (r^2) is 0.84 for the surface salinity and 0.91 for the bottom salinity (Figure 13). This indicates that the model agrees with the observed surface and bottom salinity changes over a range of salinity values.

Figures 14 and 15 show the comparison of the bottom velocity comparison for the two bottom mounted ADCPs deployed near the Edgewood Yacht Club in 2005. A series of model runs were conducted where the horizontal mixing coefficients for momentum were varied. The values coefficients were 0.01 m^2/s for NBC0705.026, 5 m^2/s NBC0705.027, and 15 m^2/s NBC0705.029. The effect of the horizontal mixing coefficient on the model output is most clearly observed in the bottom velocities in the channel (Figure 15 a,c,e). The amplitude of the north-south current velocity increases as the horizontal mixing coefficient for momentum is increased. The horizontal mixing coefficient of 15 m^2/s best matches the amplitude of the surface and bottom velocities at both the shallow and channel locations.

3.3.2 Seekonk River Model

The application of the ROMS model to the Seekonk River proved to be a challenging task. The morphology of the Seekonk includes major constrictions where simple mass conservation arguments demand significant velocity increases. Bathymetry within the upper Seekonk River varies between a relatively deep, narrow channel whose position within a given cross-section varies with axial (or longitudinal) distance along the estuary and shallow water shoals that may experience wetting/drying processes over a tidal cycle. Large flow velocity interacting with strong lateral and vertical variations in bathymetry tend to initiate numerical instabilities within the solution.

Numerical instabilities dominated the early stages of developing the Seekonk model. We experimented with different choices for time step interval and smoothing of vertical and horizontal roughness in the bathymetry. Shorter time steps are more stable but result in longer model run times (e.g., computer times) and therefore less of an ability to explore model parameter ranges (Table 4). Ultimately we settled on time steps of 5-7s (Table 4). Even with the increase in computational power provided by parallel processing this time step still results in a model that runs only approximately in real time. That is, a day of model time takes nearly a day of computer time. The time constraint placed limits on the number of long model runs conducted in the Seekonk. Smoothing of the model bathymetry was done with three passes of a Shapiro filter and was manually smoothed, particularly in the vicinity of the channel. The coastline was also manually smoothed to avoid artificial roughness that would lead to numerical instabilities. Both bathymetry and coastline smoothing was time intensive.

A number of week-long runs were completed for the period of summer 2006, followed by numerous model runs conducted over a period of four tidal cycles (Table 4). The output from the week long runs was used as the initial, starting conditions for most of the four tidal cycle model runs. Parameters that were varied to test their sensitivity on the model solutions included horizontal and vertical mixing coefficients and mixing laws, tidal forcing, river flow, bathymetry (or grid) files and different modes for applying open ocean boundary conditions (Table 4). Model output for each case was compared with velocity data (Figures 16-23) from the Seekonk ADCP deployment (discussed above; Figure 3) and salinity data (Figures 25-28) from the Phillipsdale Landing observational station within the Seekonk River.

Table 4 summarizes the set of model runs that ran successfully to completion. As part of the model development phase of the project an additional 34 partial runs were conducted which are not listed and which did not run to completion due to numerical instability. Models tested the use of simple constants for representing eddy mixing of momentum and salt as well as two types of higher order turbulence closure schemes for eddy mixing of salt and momentum, referred to as GLS (generic length scale) mixing with kappa-epsilon (KE) or kappa-omega (KO) parameterizations (see Warner et al., 2005 for discussion of GLS mixing). The choices for mixing schemes had a relatively minor impact on the resulting model-data comparisons (cases 3l versus 3m in Table 4; Figure 16 with GLS-KO versus Figure 17 with GLS-KE laws). The values for magnitudes for mixing coefficients did influence the solutions. For cases 4a-4c in Table 4, bottom versus surface salinity difference in near steady state changed from 15 ppt, 8 ppt and < 2 ppt for a Kv (vertical eddy diffusivity for salt) values of 10^{-4} , 10^{-5} and 10^{-6} m^2/s, respectively (Figure 24). Figure 29 illustrates differences in inflow/outflow velocity at a model grid station near the Seekonk ADCP deployment location, for cases 5e and 5f with identical parameters except for horizontal mixing coefficient (Kh). The run with the larger Kh (case 5f in Table 4) has a larger surface outflow during ebb. Model results show significant lateral flow structure in the solutions, even within narrow sections of the estuary such as the mouth region (e.g., the location of this data-model comparison). In the case with the lower Kh the concentrated outflow is offset from the grid location where model data is being recorded. The larger Kh smoothes out this outflow core such that ebb velocities increase at our modeled monitoring site. Based upon the literature (Warner et al., 2005) and experiences of other ROMs users (listed on the ROMS web site), we selected the GLS-KE mixing scheme for the later model runs.

Model development proceeded in multiple stages. After reaching a stage of stable model solutions and after testing different mixing conditions, we compare solutions to ADCP records from the Seekonk ADCP and surface and bottom salinity values from the Phillipsdale station. From this point the primary variables involve the runoff, tidal forcing, the conditions applied at the southern boundary and further modifications to the model grid. For the Seekonk model runs we progressed from using simplified forcing records (e.g., constant runoff, synthetic tides) to using actual data records. Therefore, data-model comparisons for velocity focus on matching the basic features of the ADCP data in terms of magnitude/duration of flood versus ebb currents and less on precise matching of the observed and modeled records in time.

One of the biggest challenges was matching the pattern in observed flood currents near the mouth of the Seekonk. Figures 16 and 17 show an overlay of modeled and observed velocity records over a 1.5 day period using model grid "shortseek". Models reproduce the basic features of the M2 tidal cycle. Maximum flood (eastward) and ebb velocity magnitudes in model and data records range from ~0.8-1 m/s. On average, the data show a broader, lower amplitude flood and a shorter duration ebb cycle. Both model runs have too much energy in the M4 frequency band. During the flood stage oscillations at this higher frequency are < 0.5 m/s whereas in the models the variations are ~0.5 to 1 m/s. A number of attempts where made to reduce the energy of oscillations at higher (M4) frequencies. Figure 18 shows a case where Kh is reduced, real runoff data is used and the M4 component of the ADCIRC tidal forcing is reduced. Here again the M4 frequency response is too large. This also results in a shortened ebb cycle relative to data (e.g., on day 4.5 in Figure 18 model currents cycle back towards flood orientations instead of progressing toward maximum ebb).

We attempted to limit the M4 response of the system by limiting the cross-sectional area of grid at the mouth (Table 4, column 10) and by trying synthetic tidal forcing functions (Table 4, column 8). Figures 19 and 20 show that this increased the velocity misfit. Utilizing narrower grid NSeek, 50% reduction in cross-sectional area, (Figure 19) and using tidal forcing with 50% larger (smaller) M2 (M4) forcing (Figure 20) leads to overly strong peek flood velocity and did not relieve the issue with shortening of the ebb through damping of M4 response in the system (e.g., days 4.5, 5.1, 5.6 in Figure 19 show the reduction in ebb velocity when data show it progressing to maximum ebb). An increase in Kh to laterally smooth out peak eastward flows had little effect (Figure 21). The bathymetry and coastline of the channel in the model grid was modified to better approximate the actual width and depth. Changes of only one grid space in this area had an effect on modeled current velocities. However, the negative influence that grid refinements had on data-model misfits can be seen by comparing cases with similar parameters but different grids (5j: Figure 22 vs. 5a Figure 17). The closest match for velocity was with the ADCIRC tidal forcing and the more diffuse grid (e.g., larger cross-sectional area).

The other aspect of the sensitivity analysis for the Seekonk modeling involved comparisons between observed and modeled salinity. The characteristics of river runoff and the southern boundary conditions, along with the vertical mixing coefficient (Figure 28) influenced salinity comparisons. The river runoff was varied in ten model runs. Initially a constant, value of 10 m^3/s was used for stability and then the actual data from summer 2006. The positions of each river had to be slightly altered to reduce the artificial salinity gradient created by introducing rivers as point sources. The Tenmile River, while not initially in the model, was added in an attempt to match surface salinity in the Seekonk. Figure 25 shows near-surface and near-bottom salinities for buoy data and the model for a case 5l. Surface values record a good match with observations in terms of the mean values and both amplitude and phase of the oscillations. The surface values range between 4 ppt and 12 ppt. The deeper comparison is not as strong. The mean values for data and model are ~13-14 ppt and 22 ppt, respectively. The tidal cycle ranges for data and model are 10 ppt and 5 ppt, respectively.

Variations in the southern boundary condition had the largest effect on the salinity of the Seekonk. The radiation boundary condition lost fresh water over the course of a tidal cycle as an artificially high salinity was defined at the boundary. Fresh water radiated out on the ebb tide, but did not return to the model domain during the flood. A salinity gradient based on the local buoy data was implemented to better represent conditions at the mouth (southern boundary) of the model. Improving the southern boundary condition resulted in significantly better matches between observed and modeled data (Figures 26 and 27), where minimum and maximum salinity values varied from 5 ppt to 10 ppt in near-surface water and between 14 ppt to 18 ppt in bear-bottom water. Changing the grid to 1m depths from 2m depths on the shallows also improved the fit between observed and modeled salinity by allowing for generally lower average water column salinities (Figure 28). Further work is needed on this, but it appears that moving towards a better representation of the near wetting/drying conditions of the shoals limits the intrusion and storage of salty water in the model simulations.

4.0 Conclusions

The boat and bottom mounted ADCP data shows the complex circulation in the Seekonk River and Upper Narragansett Bay. The bottom mounted data shows the layered flow in the Seekonk, East and West Passage channel and East Passage shoals. The flow also varied with winds and river flow. The boat mounted data captured the double flood in the West Passage and layered flow in the East Passage.

Model-data comparisons for the ROMS Providence River Model have been completed. The model adequately matches salinity observations from the Phillipsdale and North Prudence sites and current velocity near the Edgewood Yacht Club. The model is now configured to conduct experiments examining the dilution of a conservative tracer released from various point sources, such as the Field's Point treatment facility.

Modeling the Seekonk River represented a significant challenge. Significant effort went into producing grids that did not nucleate numerical instabilities. Better fits to the velocity data at the mouth were produced with a grid that was broader at the mouth, thereby producing less of a velocity increase to the water flow through a constriction. Future modeling should consider a wider range in bottom friction parameters and more detailed analysis of the horizontal mixing / turbulence closure parameters to better characterize how higher frequency (M4) energy might be damped from the solutions. Also, model runs clearly show lateral structure within the inflow/outflow fields even within narrow regions such as the location of the Seekonk ADCP. Future work should therefore include better across channel data coverage combined with more across channel model output stations. Such comparisons would allow for better understanding of how data-model misfit is influenced by meanders in concentrated inflow/outflow cores, or jets. Proper application of time series data at the southern boundary for salinity had the most important impact on reducing data-model misfit. Future work should focus on simulations of specific stratification/de-stratification events to further constrain the relative importance of vertical vs. lateral mixing and advection of water within the Seekonk. Future work should also add in the temperature field and its impact on density, stratification and long term transport processes.

5.0 References

Luettich, R.A., Westerink, J.J., ans Scheffner, N.W., 1992. *ADCIRC: An advanced three-dimensional circulation model for shelves, coasts, and estuaries*, Tech. Report DRP-92-6, U.S. Army Engineer Waterways Experiment Station, Vicksburg, MS.

Oviatt, C. A. Keller, P. Sampou, G. Almquist. 1986. Patterns of productivity during a eutrophication: a mesocosm experiment. *Mar. Ecol. Prog. Ser.* 28: 69-80.

Pawlowicz, R., B. Beardsley, and S. Lentz, "Classical tidal harmonic analysis including error estimates in MATLAB using T_TIDE", *Computers and Geosciences* 28 (2002), 929-937.

Shchepetkin, A.F. and J.C. McWilliams, 1998: Quasi-monotone advection schemes based on explicit locally adaptive dissipation, *Monthly Weather Review*, 126, 1541-1580.

Shchepetkin, A.F. and J.C. McWilliams, 2003: A Method for Computing Horizontal Pressure-Gradient Force in an Oceanic Model with a Non-Aligned Vertical Coordinate, *Journal of Geophysical Research*, 108,1-34.

Shchepetkin, A.F. and J.C. McWilliams, 2005: The Regional Ocean Modeling System: A split-explicit, free-surface, topography-following coordinates ocean model, *Ocean Modelling*, in Press

Warner, J.C, C.R. Sherwood, H.G. Arango, and R.P. Signell, 2005. Performance of Four Turbulence Closure Methods Implemented using a Generic Length Scale Method. *Ocean Modelling*, 8, 81-113.

Table 1. Location of bottom mounted ADCPs.

Station	Location	Inst. Frequency (kHz)	Depth (m)	Size of Bins (m)	Dates of Deployment
Seekonk River	41°48.973'N 71°23.379'W	1200	6	0.5	6/20-8/15/2006
West Passage Channel	41°39.869'N 71°22.292'W	300	15	1.0	6/20-10/10/2006
East Passage Channel	41°40.015'N 71°18.70'W	600	14	1.0	6/20-10/10/2006
East Passage Shallows	41°39.990'N 71°18.700'W	1200	6	0.5	8/3-9/28/2006

Table 2. Summary of underway ADCP data conducted July 11, 2006.

File #	Transect Name	Start Time (UTC)	Latitude	Longitude	End Time (UTC)	Latitude	Longitude	Tide
0	West Passage	6:47:17	41 40.0614	71 22.4257	6:56:52	41 39.7197	71 21.9743	Low
1	East Passage	7:15:00	41 40.0026	71 20.5572	7:43:14	41 39.9981	71 18.4481	
2	West Passage	8:12:46	41 40.0426	71 22.4626	8:20:54	41 39.7973	71 21.9980	
4	East Passage	8:43:21	41 40.0161	71 20.5345	9:09:18	41 39.9787	71 18.4551	
5	West Passage	9:39:45	41 39.7368	71 21.9833	9:46:40	41 40.0625	71 22.4479	
6 & 7	East Passage	10:03:13	41 40.0240	71 20.5434	10:27:05	41 39.9950	71 18.4483	
8	West Passage	11:05:15	41 39.7224	71 21.9991	11:14:13	41 40.0799	71 22.4249	
9	East Passage	11:28:34	41 40.0115	71 20.5371	11:50:52	41 39.9822	71 18.4836	High
10	West Passage	13:01:52	41 39.7276	71 21.9888	13:11:56	41 40.0699	71 22.5188	
11	East Passage	13:27:16	41 40.0823	71 20.5726	13:51:03	41 39.9663	71 18.4526	
12	West Passage	14:21:26	41 40.0566	71 22.5206	14:31:52	41 39.7393	71 21.9785	
14	East Passage	14:53:34	41 40.0110	71 20.5298	15:21:52	41 39.9613	71 18.4495	
15	West Passage	15:50:29	41 39.7484	71 22.0296	15:59:21	41 40.0725	71 22.5401	
16	East Passage	16:21:48	41 40.0369	71 20.5419	16:47:50	41 39.9553	71 18.4485	
18	West Passage	17:29:44	41 40.0609	71 22.4797	17:38:44	41 39.7276	71 21.9753	
20	East Passage	17:59:59	41 40.0428	71 20.5436	18:28:18	41 40.0004	71 18.4514	Low

Table 3. Summary of Providence River model results. Dstart: Start Date of Model Run, Open Bry: Open Boundary Conditions, Vmix v,t,turb: Vertical Mixing Coefficient for Momentum, Tracers, Turbidity (m^2/s), Hmix v,t,turb: Horizontal Mixing Coefficient for Momentum, Tracers, Turbidity (m^2/s), RGRG: Linear Bottom Drag Coefficient (m/s), zob, zos: Bottom, Surface roughness (m).

File name	Dstart	Open Bry	Vmix v	Vmix t	Vmix turb	Hmix v	Hmix t	Hmix turb	RGRG	zob	zos	Tidal Forcing	Wind Forcing	River Forcing
NBC0705.016	17-Jul	28 ppt	1.E-05	1.E-06	5.E-06	2	2	0	2.E-03	2.E-03	2.E-03	ADCIRC	Real	1x flow
NBC0705.017	17-Jul	28 ppt	1.E-05	1.E-06	2.E-06	2	2	5	2.E-03	2.E-03	2.E-03	ADCIRC	Real	1x flow
NBC0705.018	17-Jul	28 ppt	1.E-05	1.E-06	1.E-06	2	2	0	2.E-03	2.E-03	2.E-03	ADCIRC	Real	1x flow
NBC0705.019	17-Jul	28 ppt	5.E-07	5.E-07	5.E-07	1	1	0	2.E-03	2.E-03	2.E-03	ADCIRC	Real	1x flow
NBC0705.020	17-Jul	28 ppt	5.E-06	5.E-06	5.E-06	1	1	0	2.E-04	2.E-03	2.E-03	ADCIRC	Real	1x flow
NBC0705.021	17-Jul	28 ppt	5.E-06	5.E-06	5.E-06	1	1	0	2.E-04	2.E-03	2.E-03	ADCIRC	Real	1.5x flow
NBC0705.022	25-Jul	28 ppt	5.E-06	5.E-06	5.E-06	1	1	0	2.E-04	2.E-03	2.E-03	ADCIRC	Real	1.5x flow
NBC0705.023	25-Jul	28 ppt	5.E-06	5.E-06	5.E-06	1	1	0	2.E-04	2.E-03	2.E-03	ADCIRC	Real	1.5x flow
NBC0705.024	25-Jul	28 ppt	5.E-06	5.E-06	5.E-06	5	5	0	2.E-04	0	0	ADCIRC	None	1.5x flow
NBC0705.025	25-Jul	28 ppt	5.E-06	5.E-06	5.E-06	0.1	0.1	0	2.E-04	0	0	ADCIRC	None	1.5x flow
NBC0705.026	25-Jul	30 ppt	5.E-06	5.E-06	5.E-06	0.01	0.01	0	2.E-04	0	0	ADCIRC	None	1.5x flow
NBC0705.027	25-Jul	30 ppt	5.E-06	5.E-06	5.E-06	10	10	0	2.E-04	0	0	ADCIRC	None	1.5x flow
NBC0705.028	25-Jul	30 ppt	5.E-05	5.E-05	5.E-05	5	5	5	2.E-04	0	0	ADCIRC	None	1.5x flow
NBC0705.029	25-Jul	30 ppt	5.E-06	5.E-06	5.E-06	15	15	15	2.E-04	0	0	ADCIRC	None	1.5 flow
NBC0705.030	25-Jul	30 ppt	5.E-06	5.E-06	5.E-06	15	15	15	2.E-04	0	0	ADCIRC	None	Constant
NBC0705.031	25-Jul	Npru	5.E-06	5.E-06	5.E-06	15	15	15	2.E-04	0	0	ADCIRC	None	Constant
NBC0705.032	25-Jul	Npru	5.E-06	5.E-06	5.E-06	15	15	15	2.E-04	0	0	ADCIRC	None	1.5x flow
NBC0705.033	25-Jul	Npru	5.E-06	5.E-06	5.E-06	15	15	15	2.E-04	0	0	ADCIRC	None	1.5x flow
NBC0705.034	25-Jul	Npru	5.E-06	5.E-06	5.E-06	15	15	15	2.E-04	0	0	ADCIRC	Real	Constant
NBC0705.035	25-Jul	Npru	5.E-06	5.E-06	5.E-06	5	5	5	2.E-04	0	0	ADCIRC	Real	1.5x flow
NBC0705.036	25-Jul	Npru	5.E-06	5.E-06	5.E-06	5	5	5	2.E-04	0	0	No M6	Real	1.5x flow

Table 4. Summary of Seekonk River model results. Vmix V,T: Vertical mixing coefficient for momentum, tracers. Hmix T: Horizontal mixing coefficient for tracers. Closure: Vertical mixing calculation scheme. Boundary: method of enforcing given boundary conditions. River Q: Blackstone River discharge. R30 gradually ramps up river flow. Data from July and August 2006 when indicated. JA+Tenmile: Tenmile R added into model. Tides: source of or modifications to tidal elevation and current data. ADCIRC is default regional model output, ADCIRC – M4 has the M4 tidal component removed. 1.5*M2 .5*M4 strengthens the M2 and weakens the M4. Grid: Name of grid used. Grid changes are represented numerically by XC, the cross-sectional area of a north-south transect near the Seekonk ADCP location. Dt: model timestep.

Run	Vmix T	Vmix V	Hmix T	Closure	Boundary	River Q	Tides	Grid	XC	Dt
	m^2/sec	m^2/sec	m^2/sec			m^3/sec			M^3	Sec
3d	1E-4	1E-4	1E-2	GLS – KO	Radiation	R30	ADCIRC	Shortseek	1016.5	5
3e	1E-4	1E-4	1E-2	GLS – KO	Radiation	15	ADCIRC	Shortseek	1016.5	5
3f	1E-3	1E-3	1E-2	GLS – KO	Radiation	R30	ADCIRC	Shortseek	1016.5	5
3g	1E-5	1E-5	1E-2	GLS – KO	Radiation	R30	ADCIRC	Shortseek	1016.5	5
3h	5E-5	5E-5	1E-2	GLS – KO	Radiation	10	ADCIRC	Shortseek	1016.5	5
3i	1E-5	5E-5	1E-2	GLS – KO	Radiation	10	ADCIRC	Shortseek	1016.5	5
3j	1E-5	5E-5	1E-2	GLS – KO	Radiation	10, 10PSU	ADCIRC	Shortseek	1016.5	5
3k	1E-5	1E-5	1E-2	GLS – KO	Radiation	10, 10PSU	ADCIRC	Shortseek	1016.5	5
3l	1E-5	1E-5	1E-2	GLS – KO	Radiation	10, 10PSU	ADCIRC – M4	Shortseek	1016.5	5
3m	1E-6	1E-6	0E+0	GLS – KE	Radiation	10	ADCIRC – M4	Shortseek	1016.5	5
4a	1E-4	1E-4	1E+1	Constant	Radiation	10	1.5*M2 .5*M4	Shortseek	1016.5	5
4b	1E-5	1E-5	1E+1	Constant	Radiation	10	1.5*M2 .5*M4	Shortseek	1016.5	5
4c	1E-6	1E-6	1E+1	Constant	Radiation	10	1.5*M2 .5*M4	Shortseek	1016.5	5
4d	1E-4	1E-4	1E+1	Constant	Radiation	10	1.5*M2 .5*M4	Shortseek	1016.5	5
4e	1E-4	1E-4	1E-2	Constant	Radiation	10	1.5*M2 .5*M4	Shortseek	1016.5	5
4f	1E-4	1E-4	0E+0	Constant	Radiation	10	1.5*M2 .5*M4	Shortseek	1016.5	5
5a	1E-6	1E-6	0E+0	GLS – KE	Radiation	10	ADCIRC – M4	Shortseek	1016.5	5
5b	1E-6	1E-6	0E+0	GLS – KE	Radiation	Jul-Aug06	ADCIRC – M4	Shortseek	1016.5	7
5c	1E-6	1E-6	1E+0	GLS – KE	Radiation	Jul-Aug06	ADCIRC – M4	Shortseek	1016.5	7
5d	1E-6	1E-6	1E+0	GLS – KE	Radiation	Jul-Aug06	ADCIRC – M4	Nseek	531	7
5e	1E-6	1E-6	1E+0	GLS – KE	Radiation	Jul-Aug06	1.5*M2 .5*M4	Nseek	531	7
5f	1E-6	1E-6	2E+0	GLS – KE	Radiation	Jul-Aug06	1.5*M2 .5*M4	Nseek	531	7
5g	1E-6	1E-6	2E+0	GLS – KE	Radiation	JA+Tenmile	1.5*M2 .5*M4	Nseek	531	7
5h	1E-7	1E-7	2E+0	GLS – KE	Radiation	JA+Tenmile	1.5*M2 .5*M4	Nseek	531	7
5i	1E-7	1E-7	2E+0	GLS – KE	Radiation	JA+Tenmile	1.5*M2 .5*M4	Nseek	531	7
5j	1E-7	1E-7	2E+0	GLS – KE	Radiation	JA+Tenmile	ADCIRC – M4	Nseek	531	7
5k	1E-7	1E-7	2E+0	GLS – KE	Radiation	JA+Tenmile	ADCIRC – M4	Nseek	531	7
5l	1E-7	1E-7	2E+0	GLS – KE	Radiation	JA+Tenmile	ADCIRC – M4	Nseek	531	7
5m	1E-7	1E-7	2E+0	GLS – KE	Radiation	JA+Tenmile	ADCIRC – M4	Nseek	531	7
5n	1E-7	1E-7	2E+0	GLS – KE	Radiation	JA+Tenmile	ADCIRC – M4	Nseek	531	7
5o	1E-7	1E-7	2E+0	GLS – KE	Radiation	JA+Tenmile	ADCIRC – M4	Nseek	531	7
5p	1E-7	1E-7	2E+0	GLS – KE	Radiation	JA+Tenmile	ADCIRC – M4	Nseek2	484	7
6b	1E-7	1E-7	2E+0	GLS – KE	Nudging	JA+Tenmile	ADCIRC – M4	Nseek2	484	7
6c	1E-7	1E-7	2E+0	GLS – KE	Clamped	JA+Tenmile	ADCIRC – M4	Nseek2	484	7
6d	1E-7	1E-7	2E+0	GLS – KE	Clamped	JA+Tenmile	ADCIRC – M4	Seek1m	675	7
6e	1E-7	1E-7	2E+0	GLS – KE	Clamped	JA+Tenmile	ADCIRC – M4	Seek1m	675	7
6f	1E-7	1E-7	2E+0	GLS – KE	Clamped	JA+Tenmile	ADCIRC	Seek1m	675	7

Comments: 5d – New grid with smaller Seekonk channel. 5h – 5k were tide timing and model restart tests. 5l-5m were fine-tuning river input locations. 5n took boundary salinity from Bullock Reach buoy. 5o-5p used buoy data to improve initial conditions and new grid with smoother Seekonk channel. 6d – new grid with minimum depth reduced from 2m to 1m.

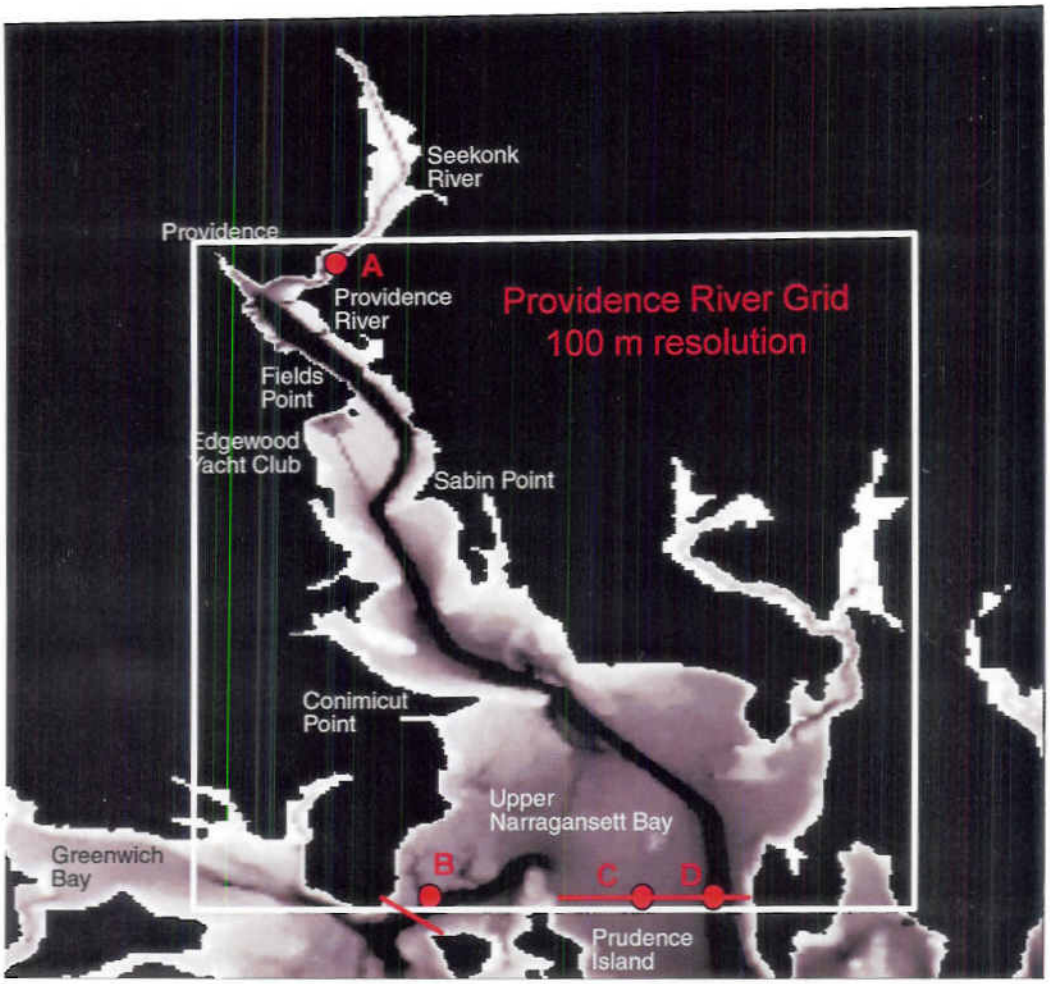

Figure 1. Map showing the study area of Providence River, RI. Locations of four bottom mounted ADCPs used in this study are shown (red dots): A- Seekonk River, B- West Passage Channel, C- East Passage Channel, and D- East Passage Shallows. The underway survey lines are also shown (red lines). Bathymetry is represented in grey scale (darker grey=deeper water). The white box represents the ROMS model domain.

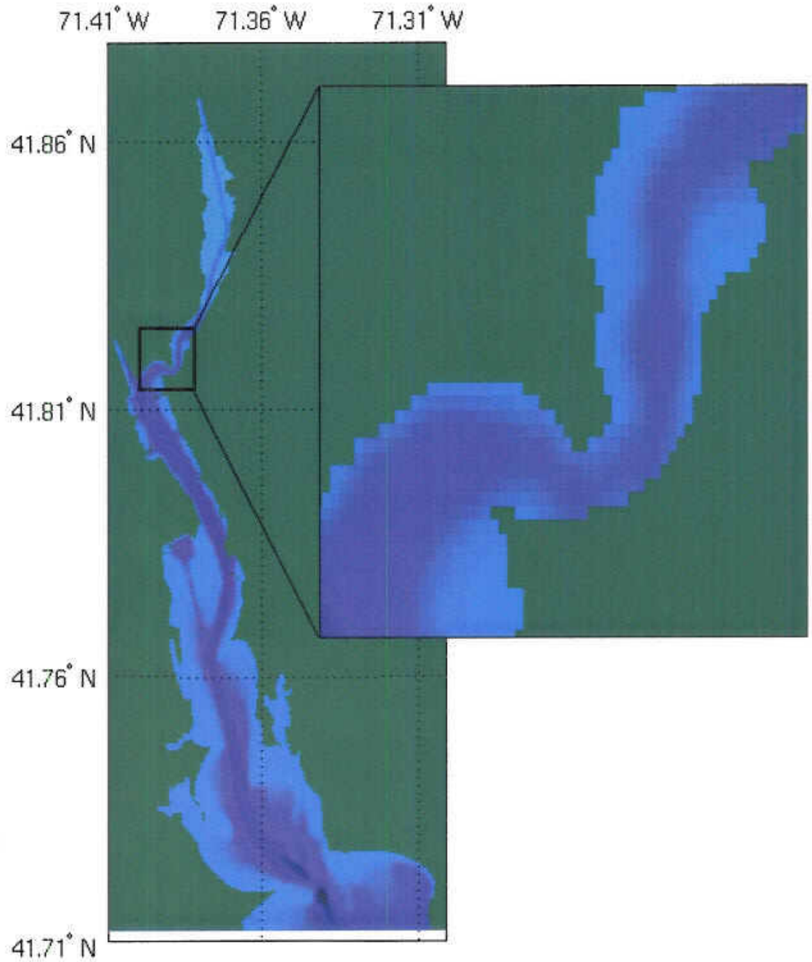

Figure 2. Map showing the domain of the Seekonk River model.

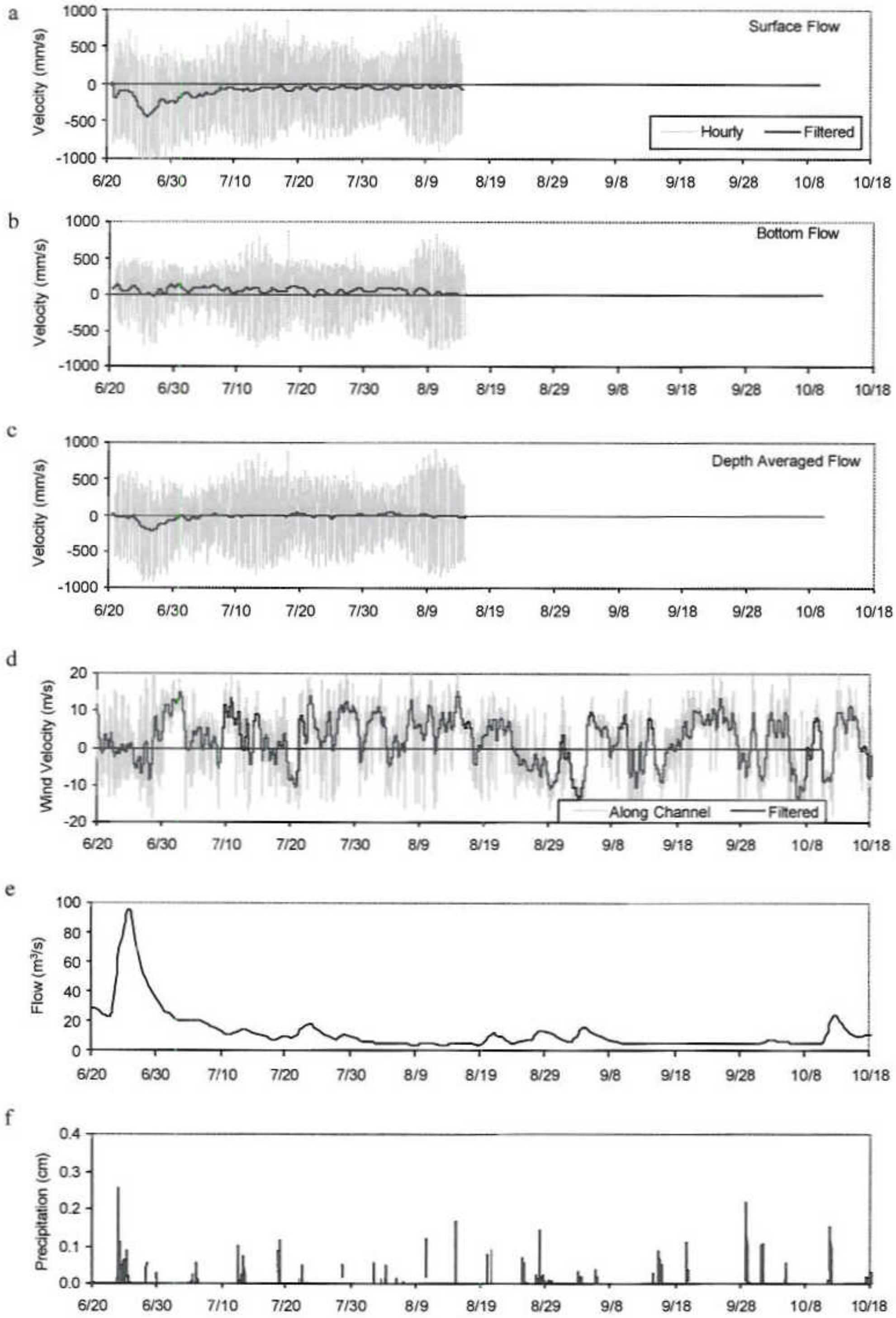

Figure 3. Bottom mounted data from Seekonk River (1200kHz ADCP), (a) near-surface inflow (+) and outflow (-), (b) near-bottom inflow and outflow, (c) depth averaged inflow and outflow, (d) T.F. Green along channel wind velocity (up channel (+) and down channel (-)), (e) Blackstone River flow and (f) T.F. Green precipitation.

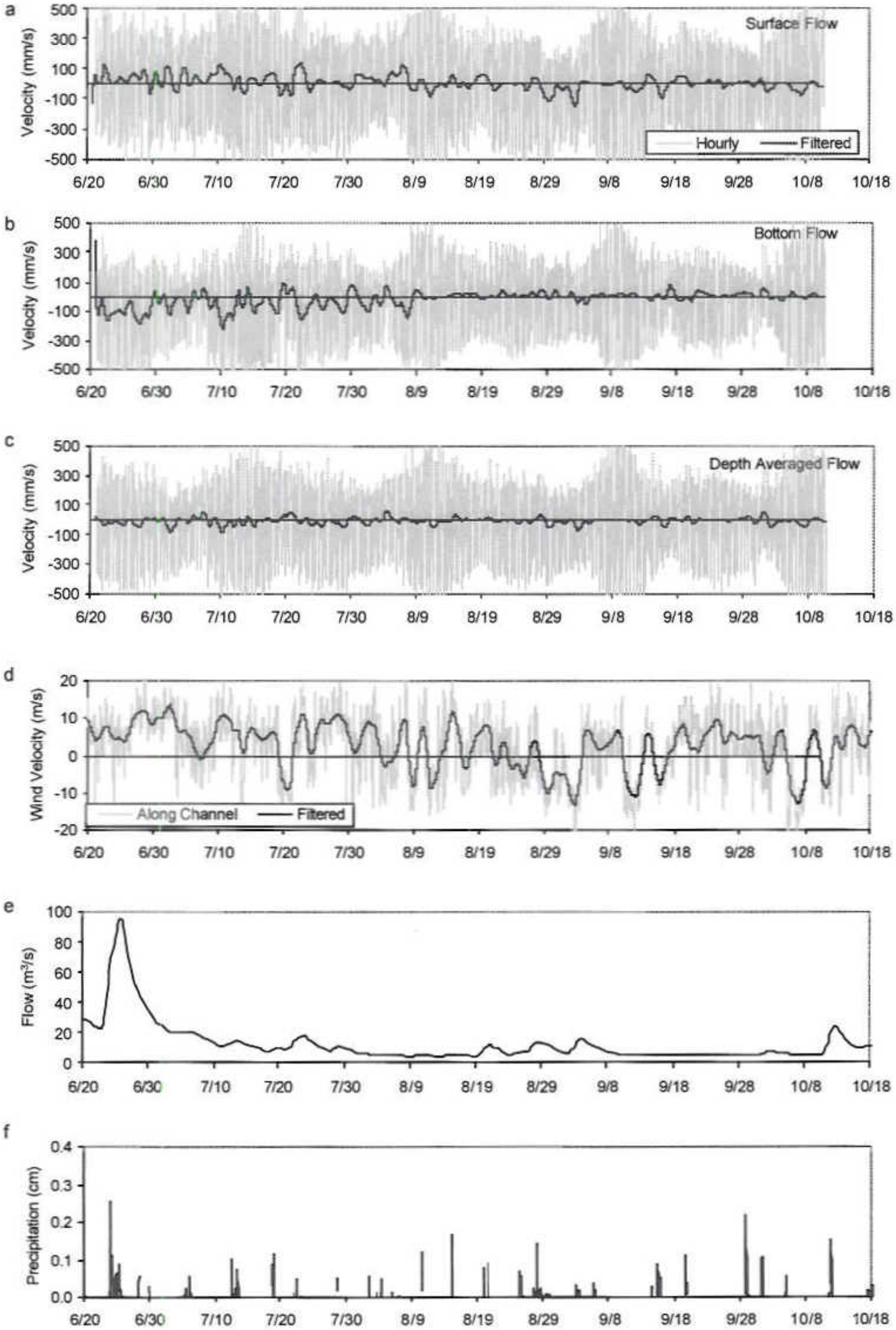

Figure 4. Bottom mounted data from the West Passage Channel (300kHz ADCP), (a) near-surface inflow (+) and outflow (-), (b) near-bottom inflow and outflow, (c) depth averaged inflow and outflow, (d) T.F. Green along channel wind velocity (up channel (+) and down channel (-)), (e) Blackstone River flow and (f) T.F. Green precipitation.

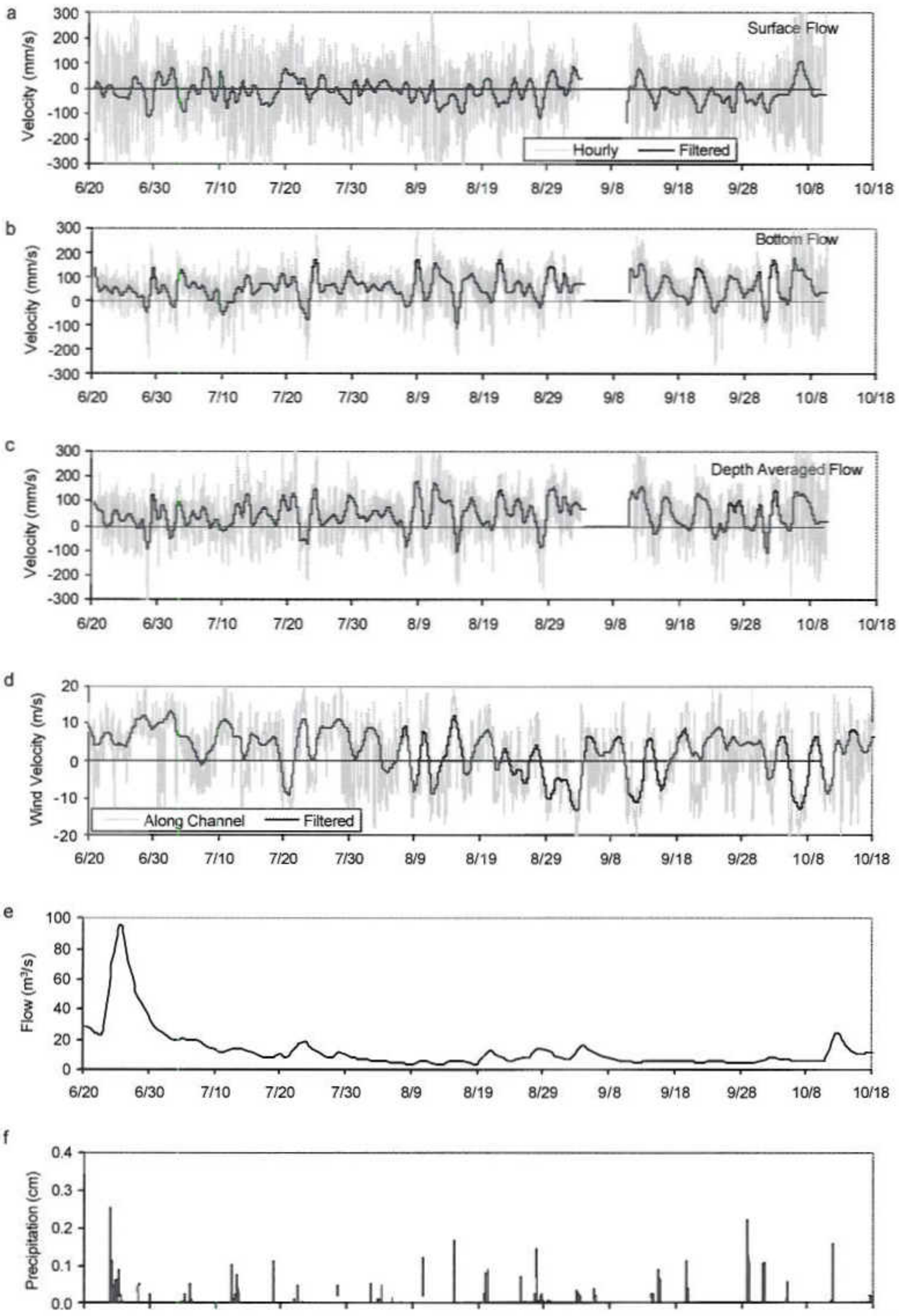

Figure 5. Bottom mounted data from the East Passage Channel (600kHz ADCP), (a) near-surface inflow (+) and outflow (-), (b) near-bottom inflow and outflow, (c) depth averaged inflow and outflow, (d) T.F. Green along channel wind velocity (up channel (+) and down channel (-)), (e) Blackstone River flow and (f) T.F. Green precipitation.

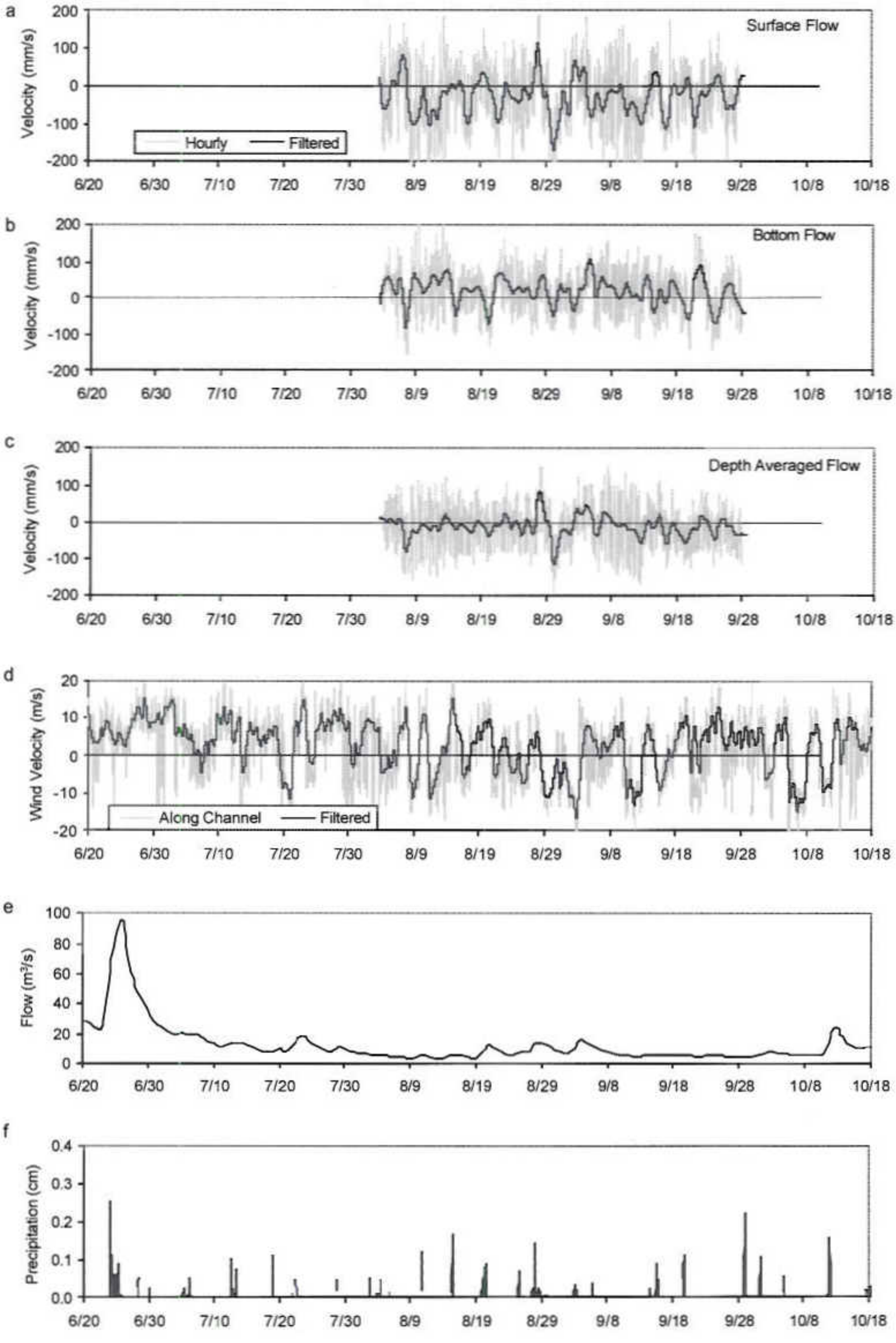

Figure 6. Bottom mounted data from the East Passage Shallows (1200kHz ADCP), (a) near-surface inflow (+) and outflow (-), (b) near-bottom inflow and outflow, (c) depth averaged inflow and outflow, (d) T.F. Green along channel wind velocity (up channel (+) and down channel (-)), (e) Blackstone River flow and (f) T.F. Green precipitation.

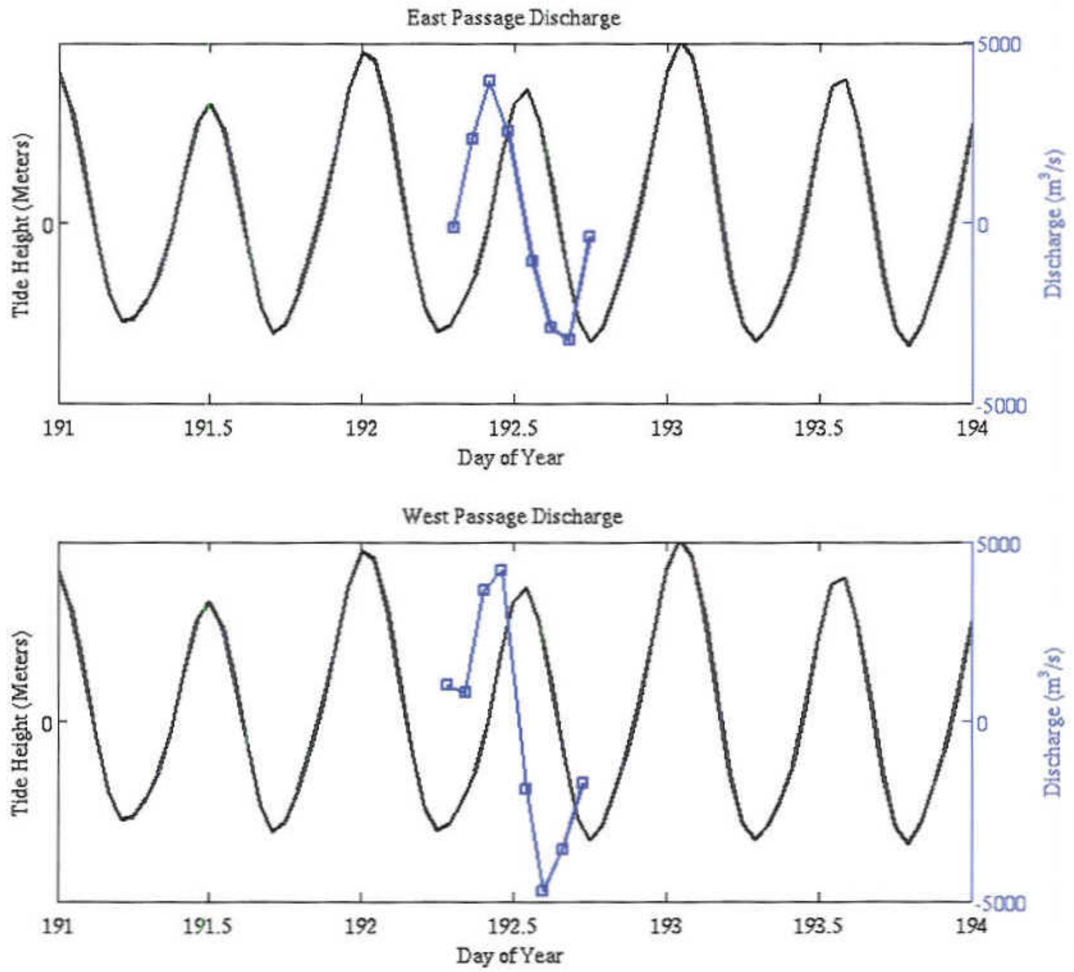

Figure 7. Discharge through the East and West Passage transects on July 11, 2006.

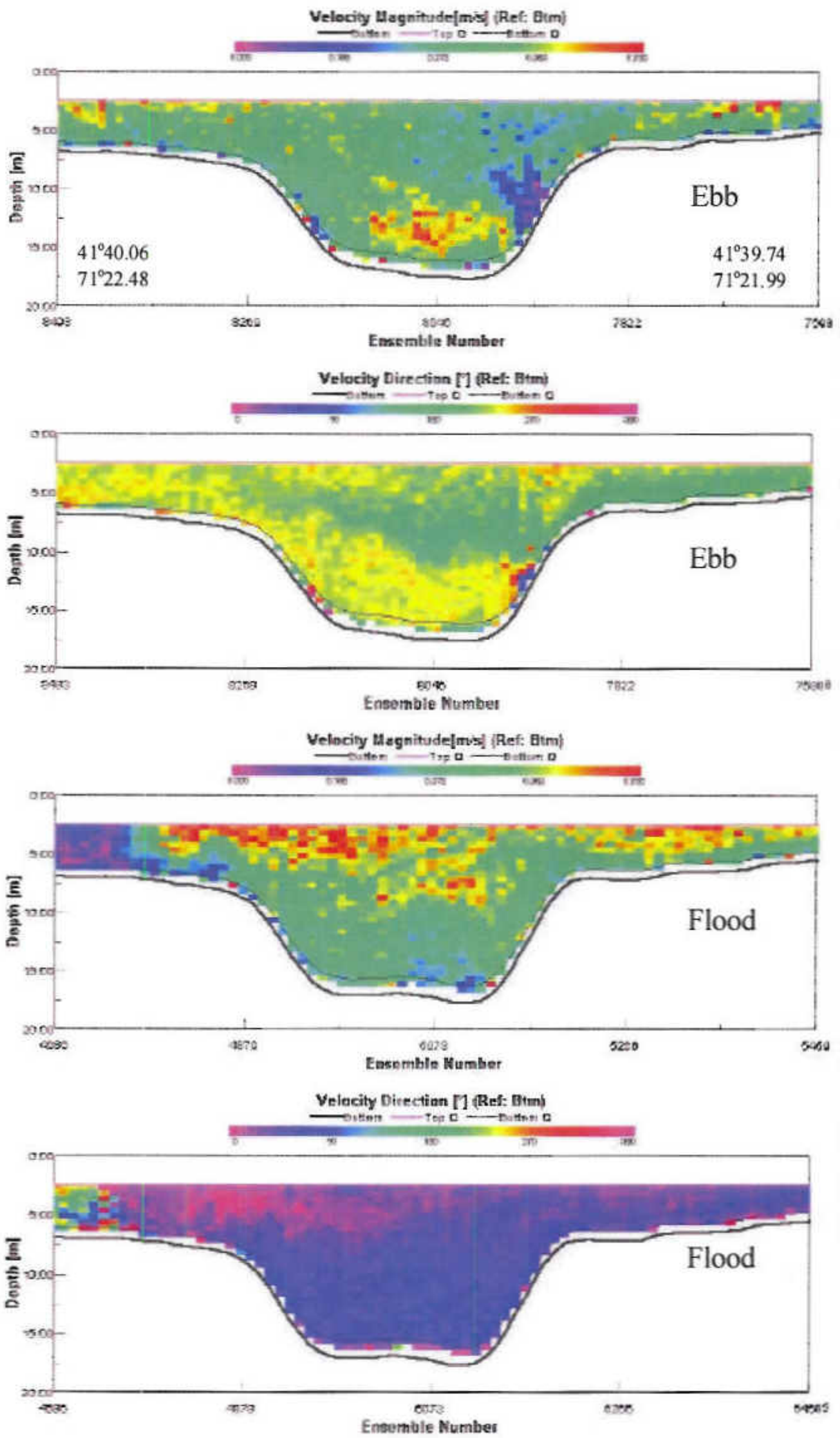

Figure 8. Flow patterns through the West Passage during the ebb and flood tides.

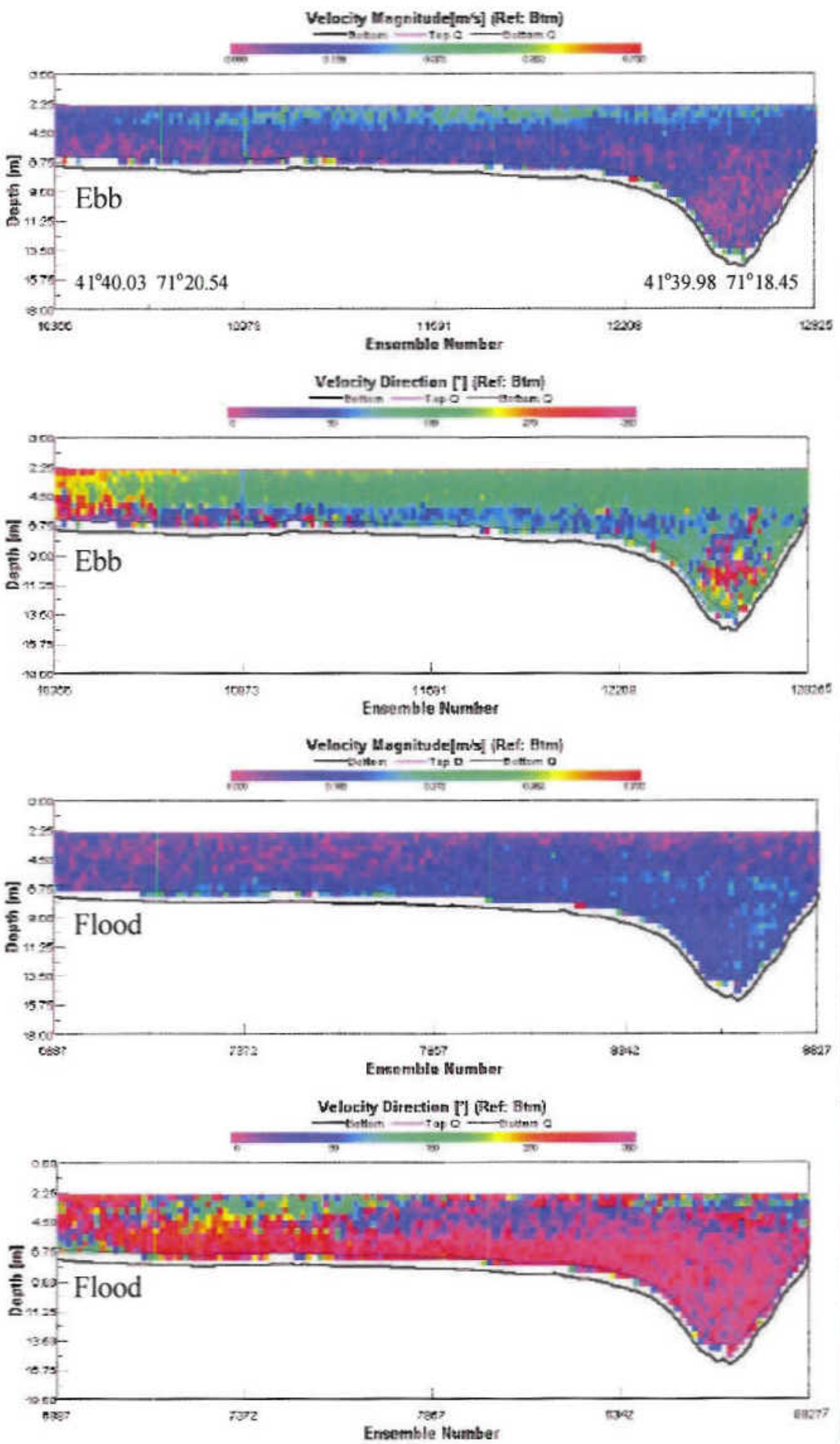

Figure 9. Flow patterns through the East Passage during the ebb and flood tides.

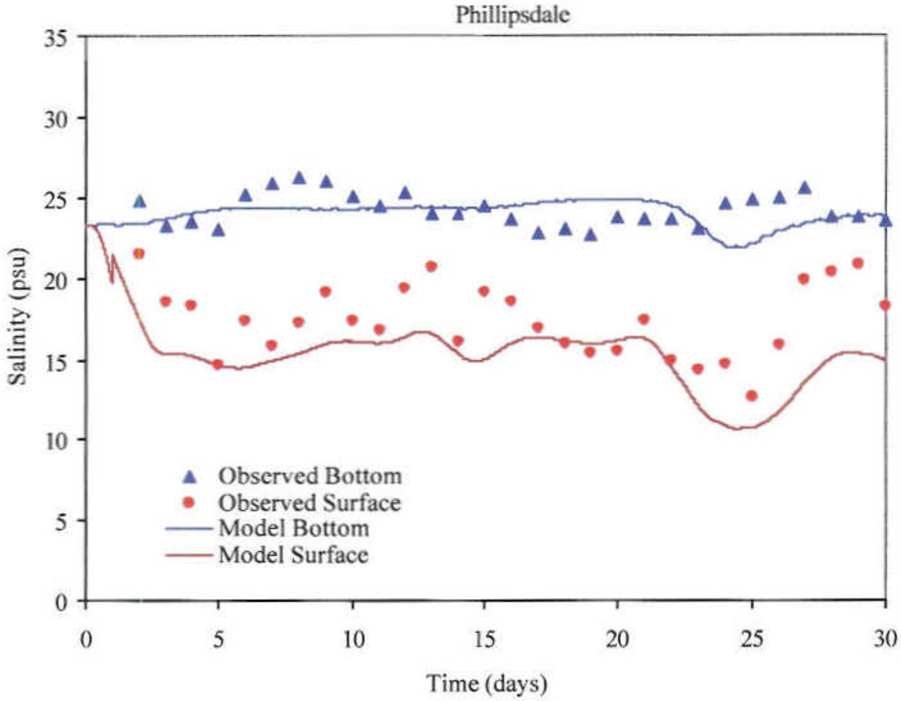

Figure 10. Model-data comparison for Phillipsdale monitoring station for model run NBC-0705.021. The surface values are in red, bottom values in blue. The solid lines represent the model results.

a.

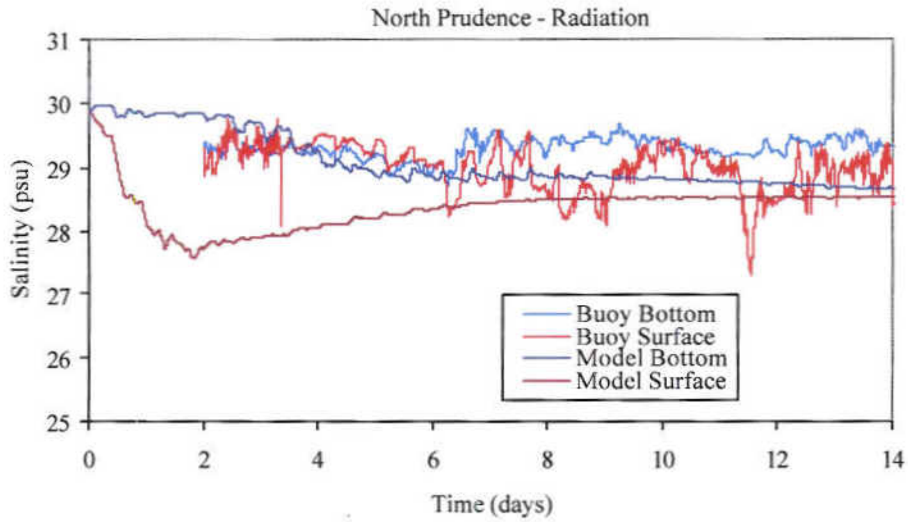

b.

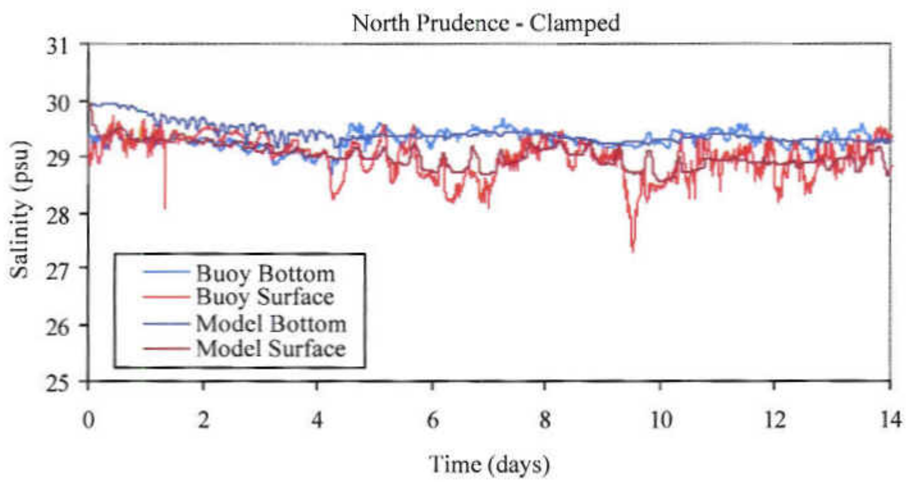

Figure 11. Model-data comparison of salinity from the North Prudence Buoy, during July 2005 for differing boundary conditions (a) radiation conditions (NBC0705.024) and (b) clamped (NBC0705.035).

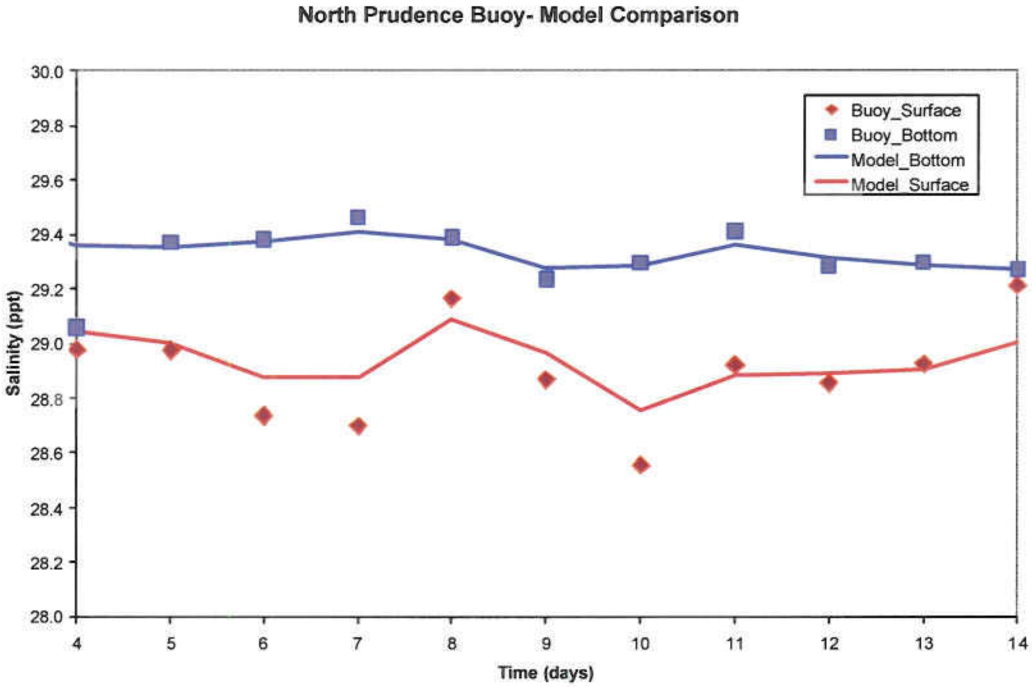

Figure 12. Model-data comparison of salinity from the North Prudence Buoy, during July 2005. The surface values are in red and the bottom values are in blue. Buoy data are shown as points and model output as lines.

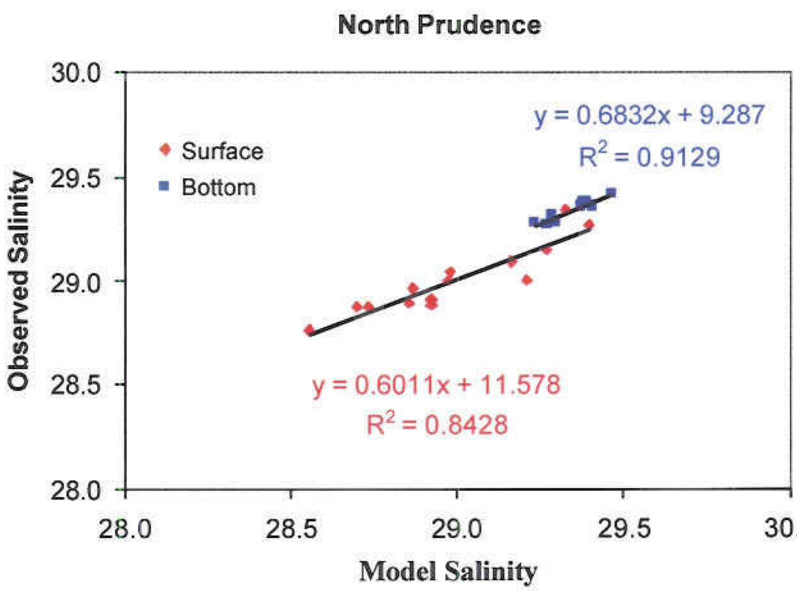

Figure 13. Linear regression of the model-data comparison of salinity from the North Prudence buoy.

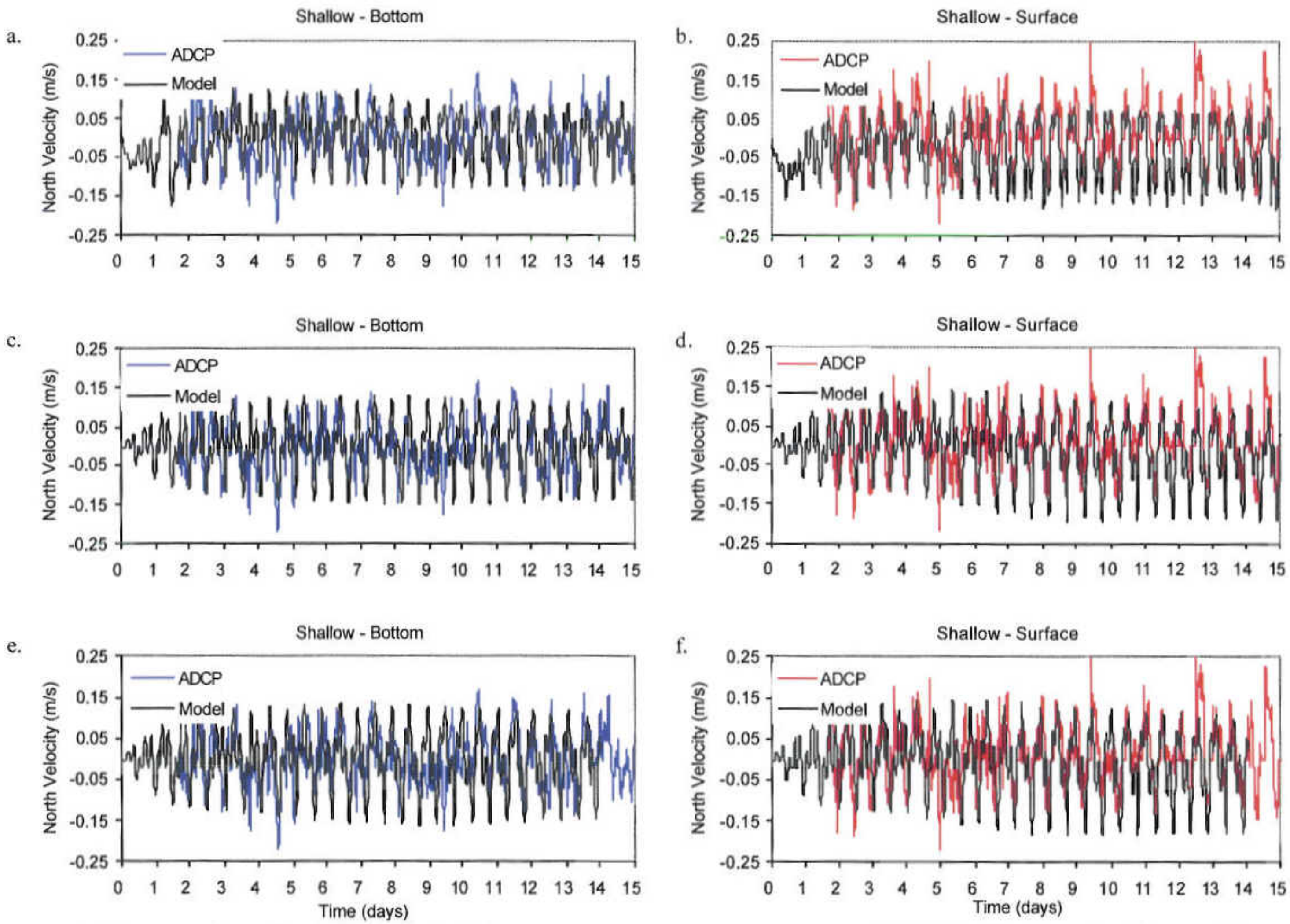

Figure 14. Model-data comparison of velocity from the Edgewood Yacht Club shallows, during July 2005 a) horizontal mixing coefficient for momentum of 0.01 m^2/s for bottom velocity, b) surface velocity, c) horizontal mixing coefficient for momentum of 5 m^2/s for bottom velocity, d) surface velocity, e) horizontal mixing coefficient for momentum of 15 m^2/s for bottom velocity, and f) surface velocity,

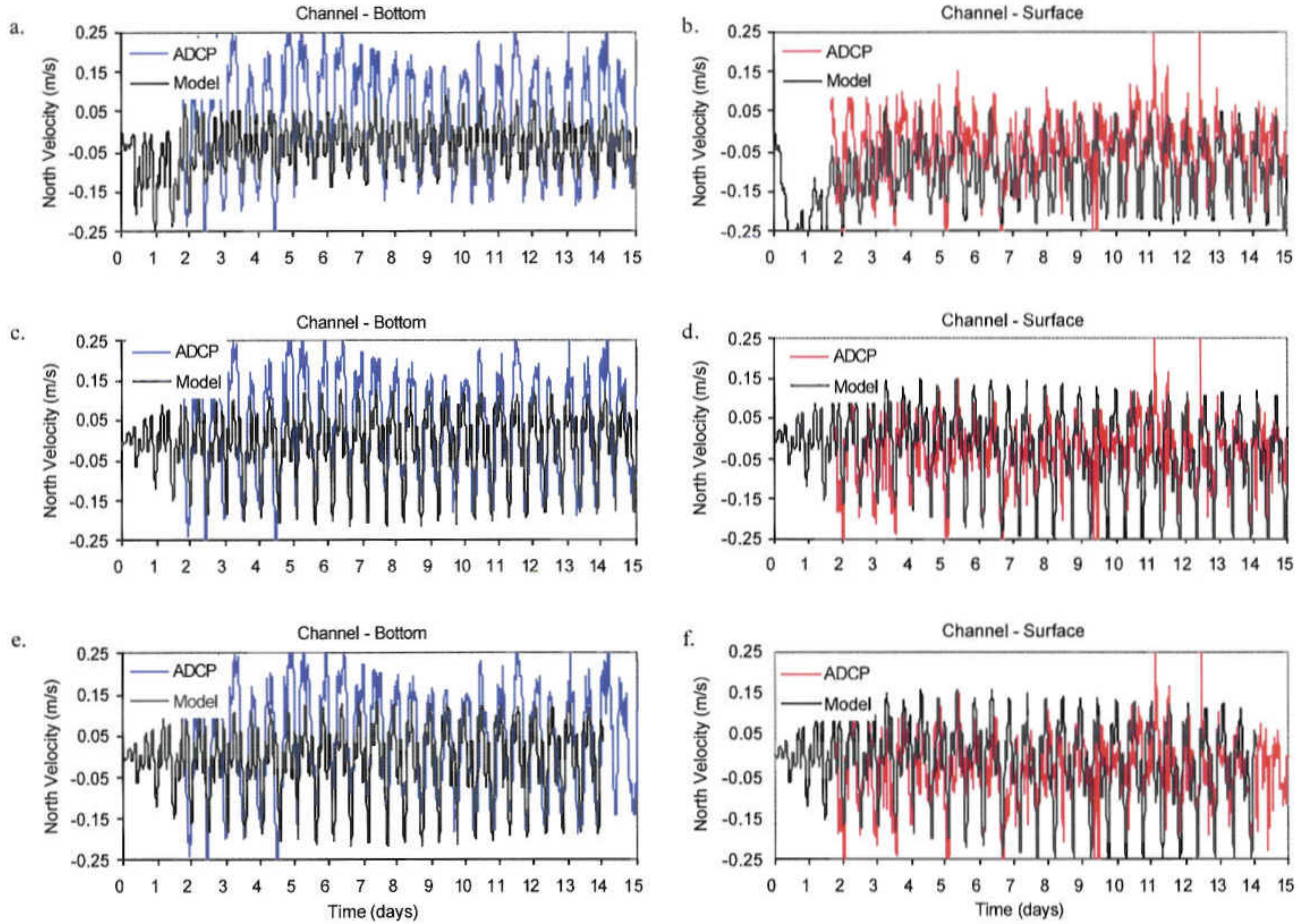

Figure 15. Model-data comparison of velocity from the Edgewood Yacht Club channel, during July 2005 a) horizontal mixing coefficient for momentum of 0.01 m^2/s for bottom velocity, b) surface velocity, c) horizontal mixing coefficient for momentum of 5 m^2/s for bottom velocity, d) surface velocity, e) horizontal mixing coefficient for momentum of 15 m^2/s for bottom velocity, and f) surface velocity,

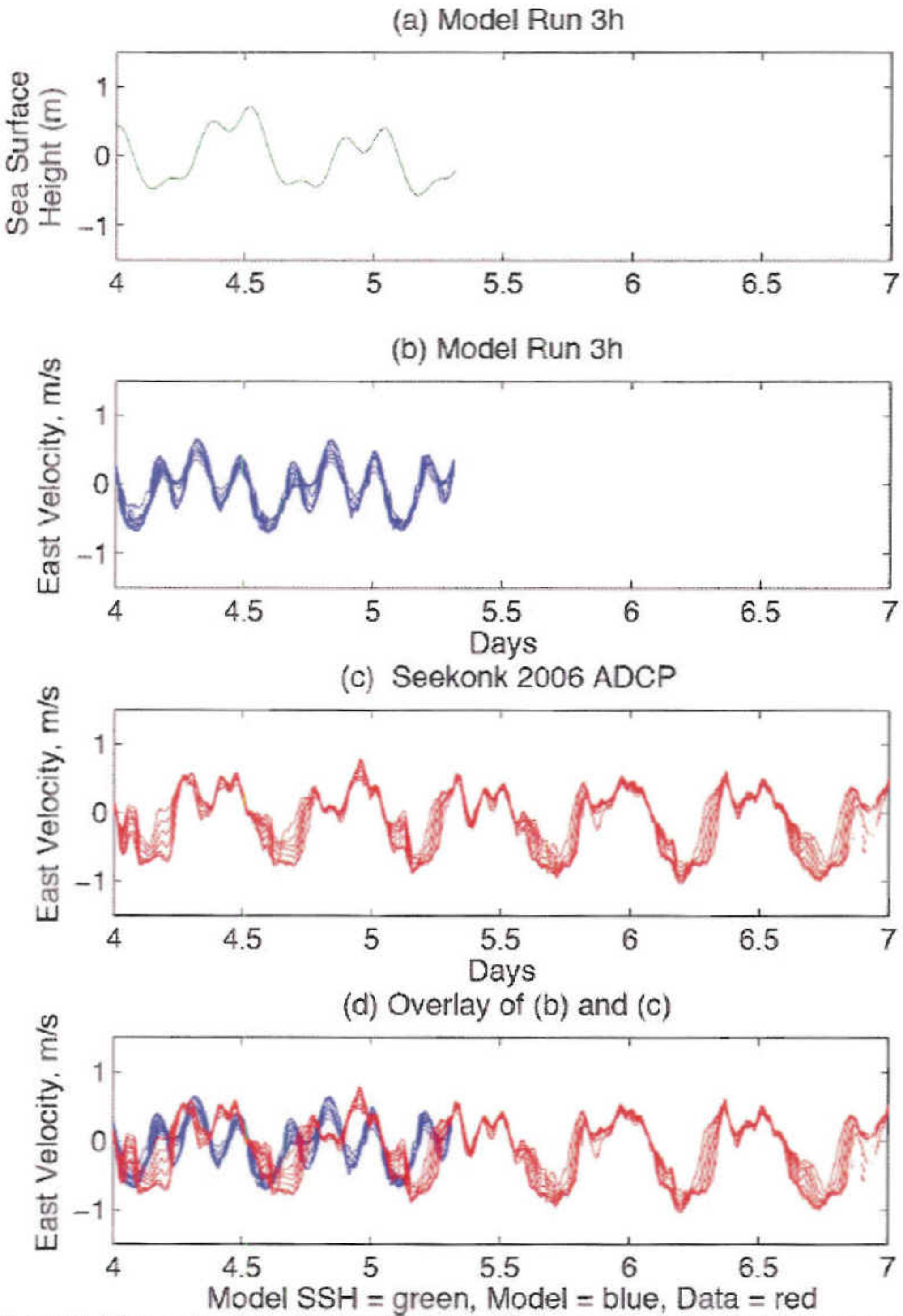

Figure 16. Time series plots of sea surface height (a) and eastward (flooding) and westward (ebbing) velocity for model run 3h (Table 4). Plots are shown for ADCP data (Figure 1) and from a point (or station) within the numerical grid that corresponds to the ADCP location at the mouth of the Seekonk RIver, shown in Figure 1.

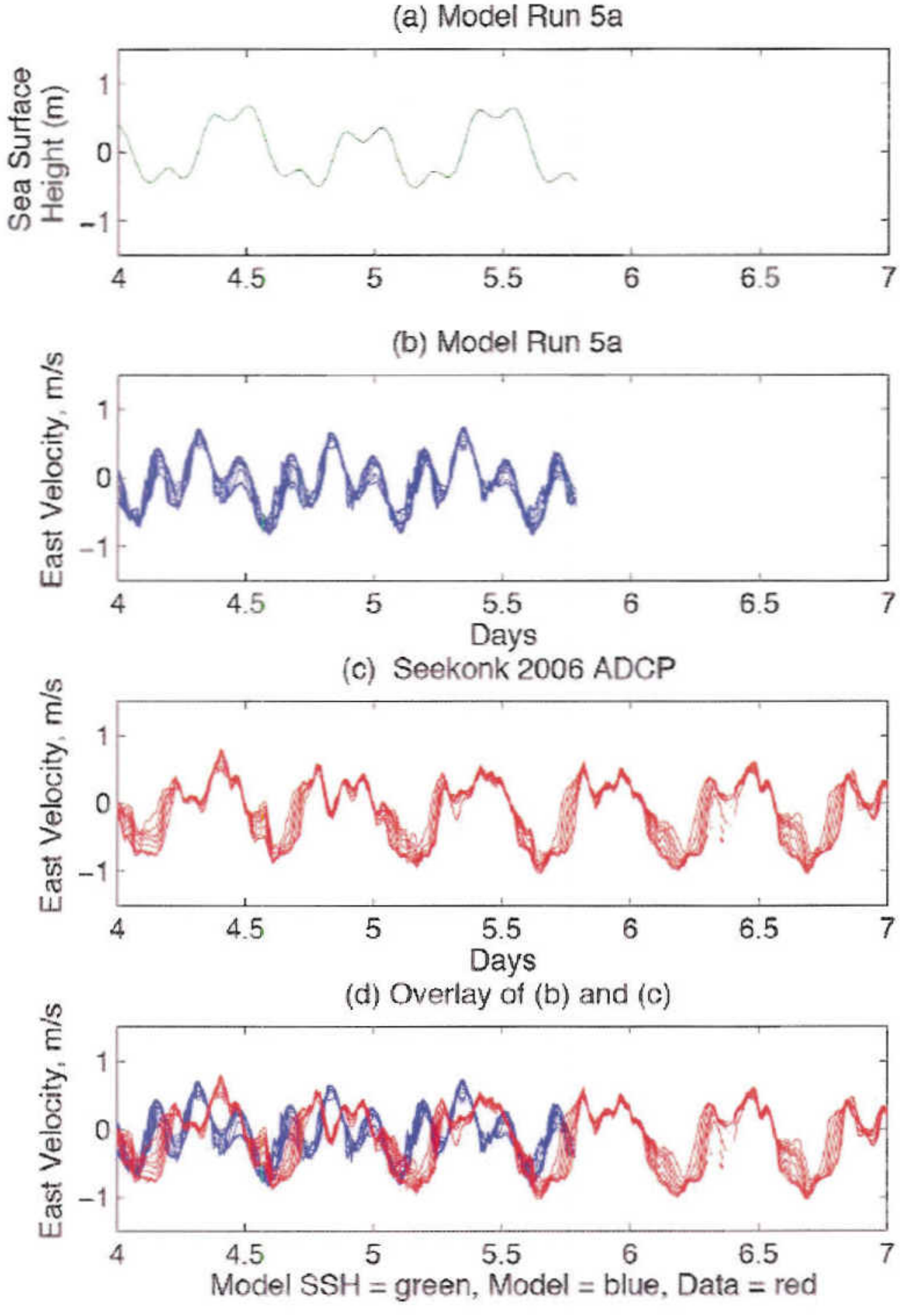

Figure 17. Similar time series plots to Figure 16, but for model run 5a (Table 4). The mixing scheme has changed from GLS-KO to GLS-KE and the vertical (horizontal) mixing parameters are increased (decreased) relative to Figure 16. In this case the M4 component of the ADCIRC tidal forcing has been reduced.

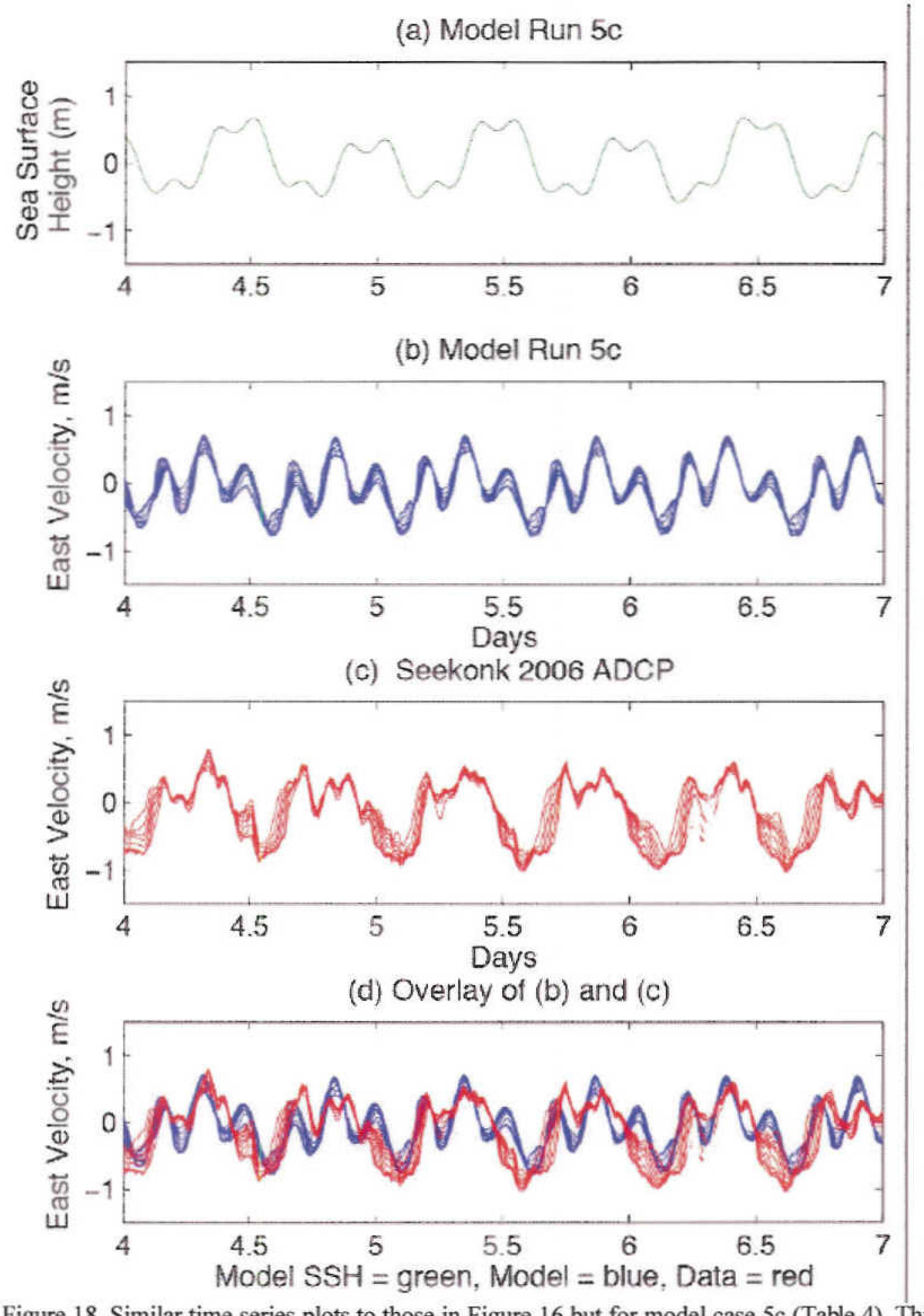

Figure 18. Similar time series plots to those in Figure 16 but for model case 5c (Table 4). This case is identical to 5a in Figure 17 except for a larger horizontal mixing parameter (Kh of 1 m^2/s versus 0.02 m^2/s).

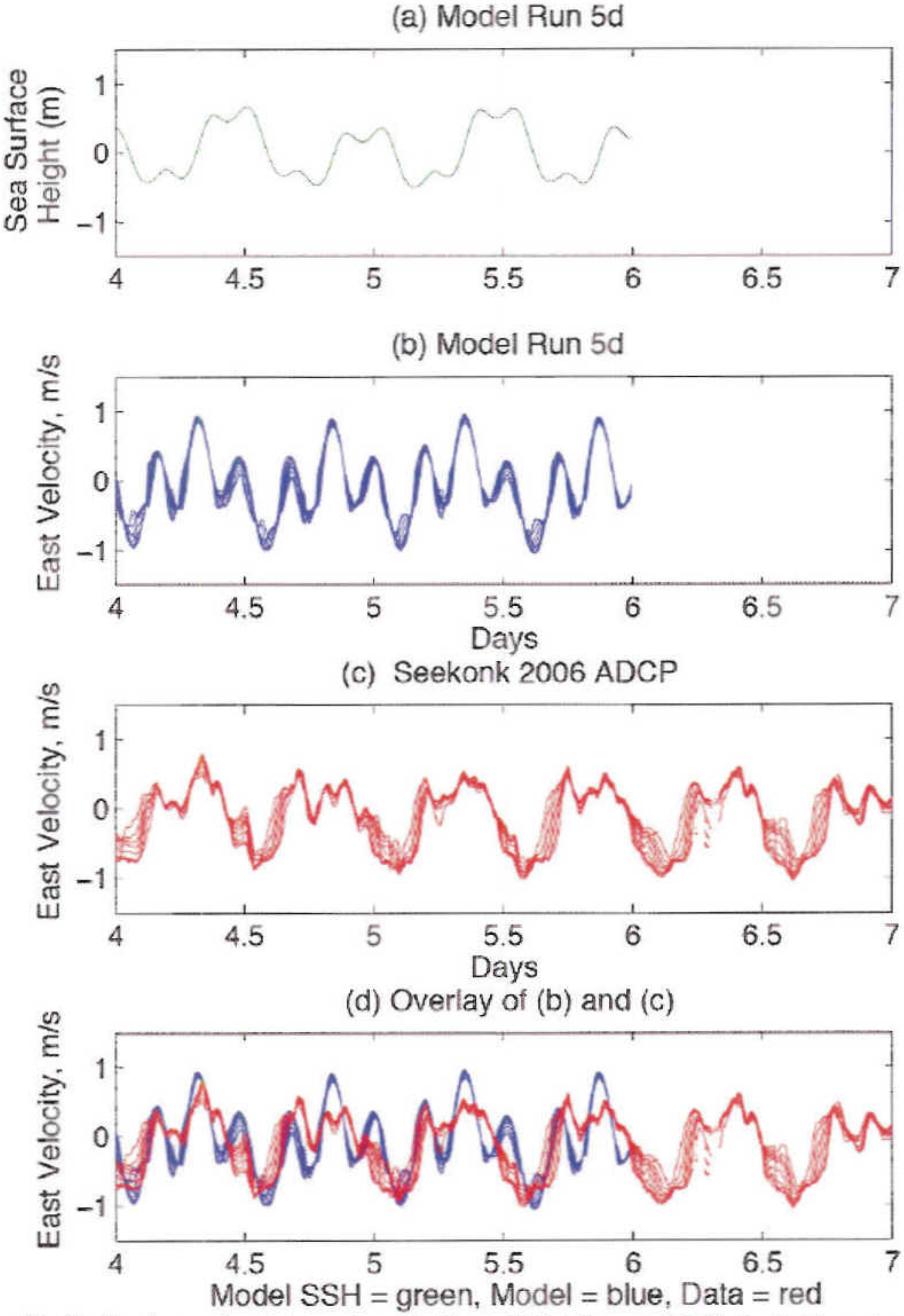

Figure 19. Similar time series plots as shown in Figure 16 but for case 5d (Table 4). The primary difference is a change in the bathymetric grid. Here the grid attempts to represent some of the finer scale features of the Seekonk, including a 50% reduction in cross-sectional area at the mouth of the river, in the vicinity of the ADCP station and the corresponding station for model output. Here the peak flood velocities begin to exceed observed values.

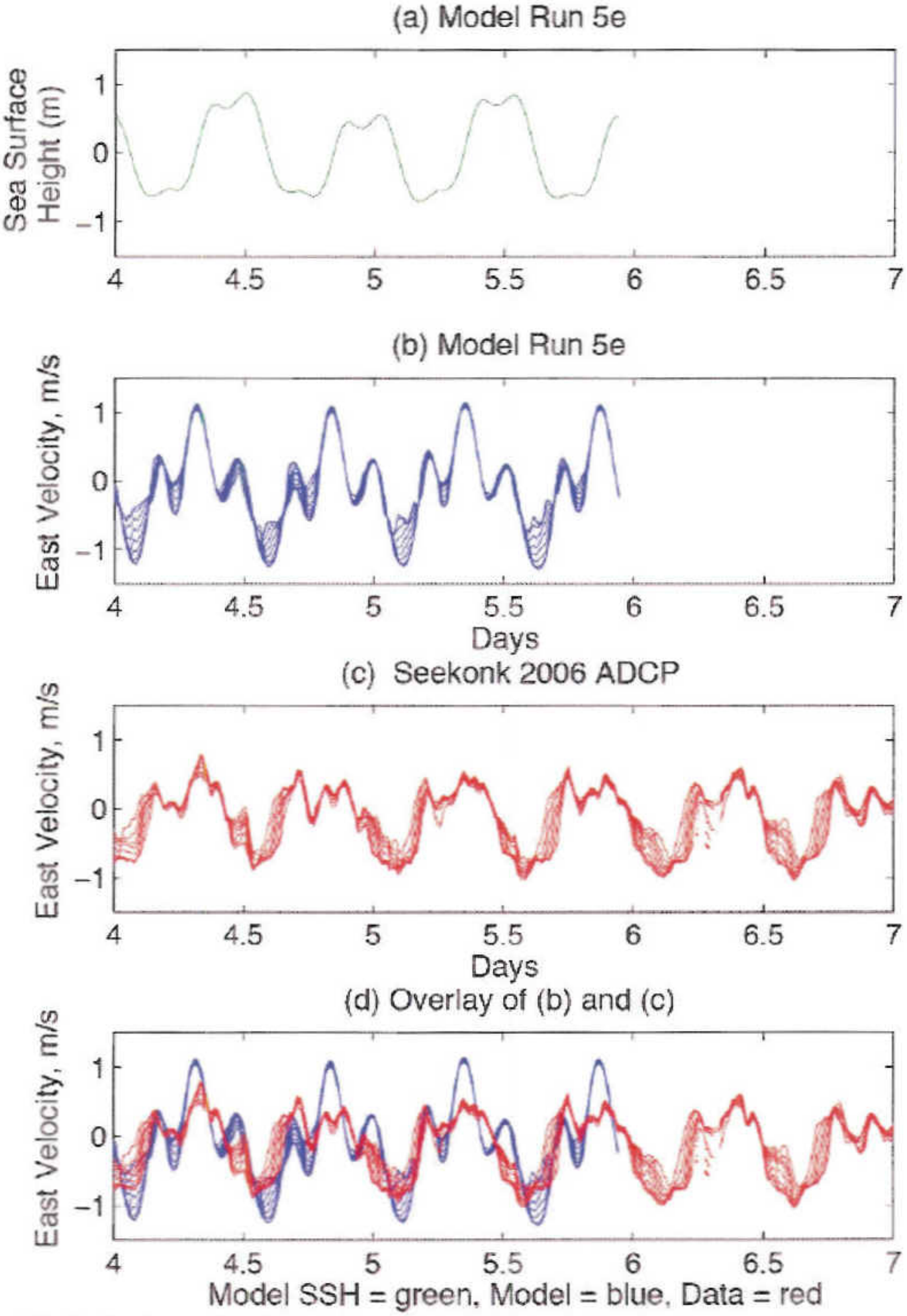

Figure 20. Similar time series plots to those shown in Figure 16 but for case 5e. This run is identical to that shown in Figure 19, but with a new synthetic formulation for tidal forcing. The ADCIRC model is replaced with a parameterization that increases the M2 component by 50% and reduces the M4 component by 50%. This results in a larger overestimate of peak flood velocity and a poorer fit with data.

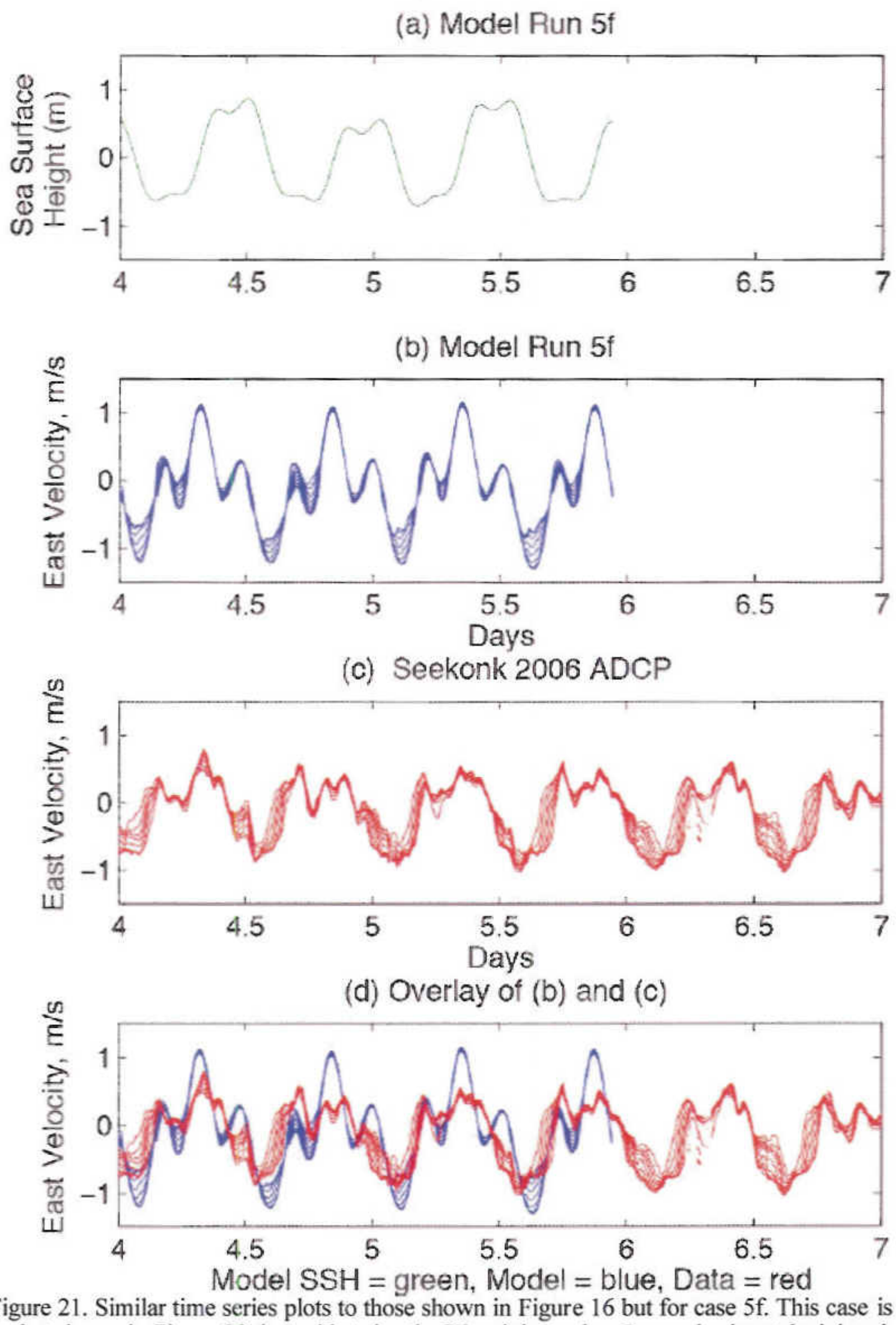

Figure 21. Similar time series plots to those shown in Figure 16 but for case 5f. This case is identical to that shown in Figure 20, but with twice the Kh mixing value. Larger horizontal mixing does not fix the mismatch in peak flood velocities and makes for a poorer fit with peak ebb velocities. Larger Kh values appear to allow more of the maximum inflow/outflow jet to be sampled at this station by laterally smoothing the velocity field.

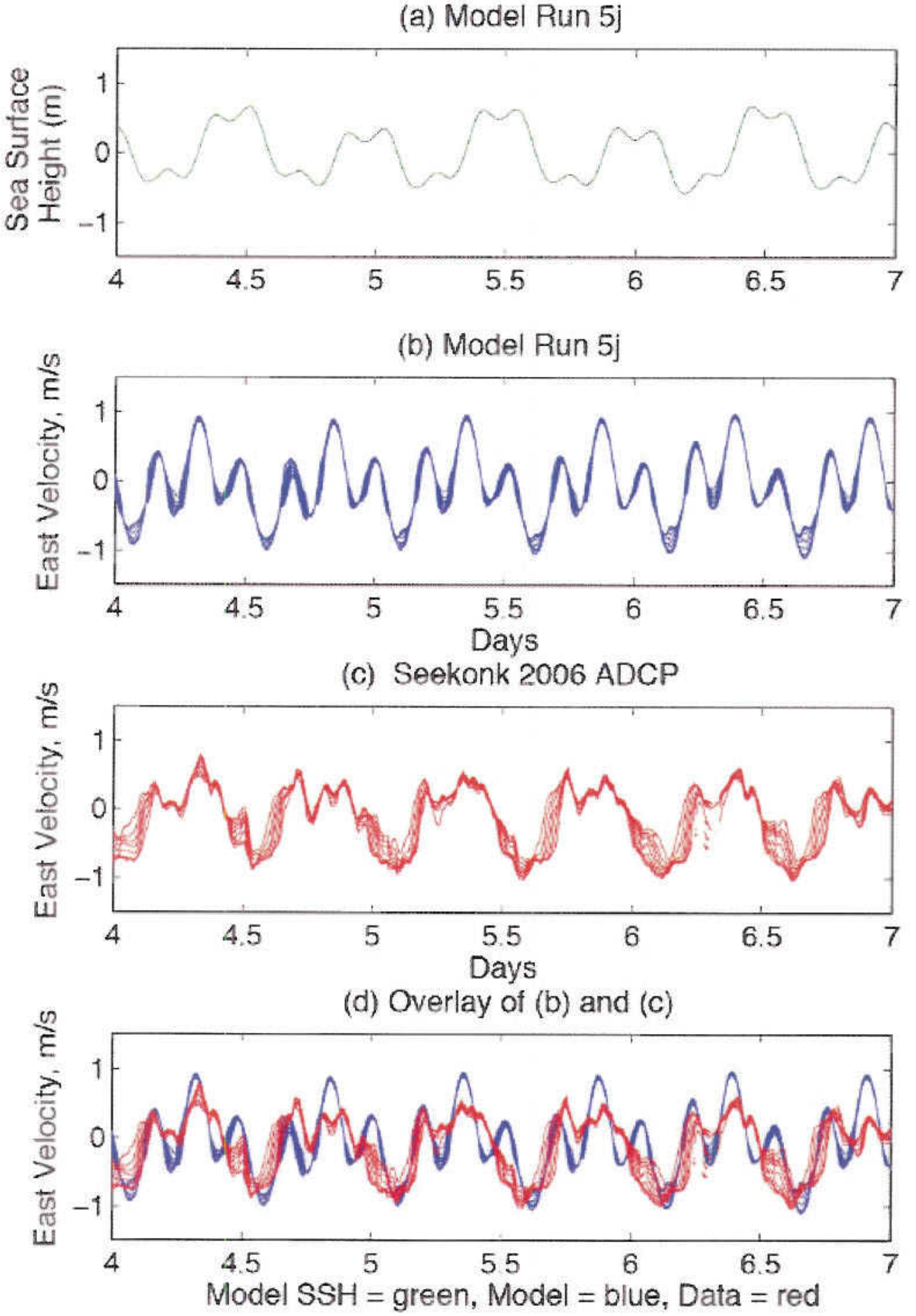

Figure 22. Similar time series plots to those shown in Figure 16 but for case 5j. This case shows the important effect of tidal forcing. This case is similar to Figure 21, but with the tidal forcing returned to the ADCIRC model with a reduced M4 constituent. Modeled ebb flow rates are more in line with observed.

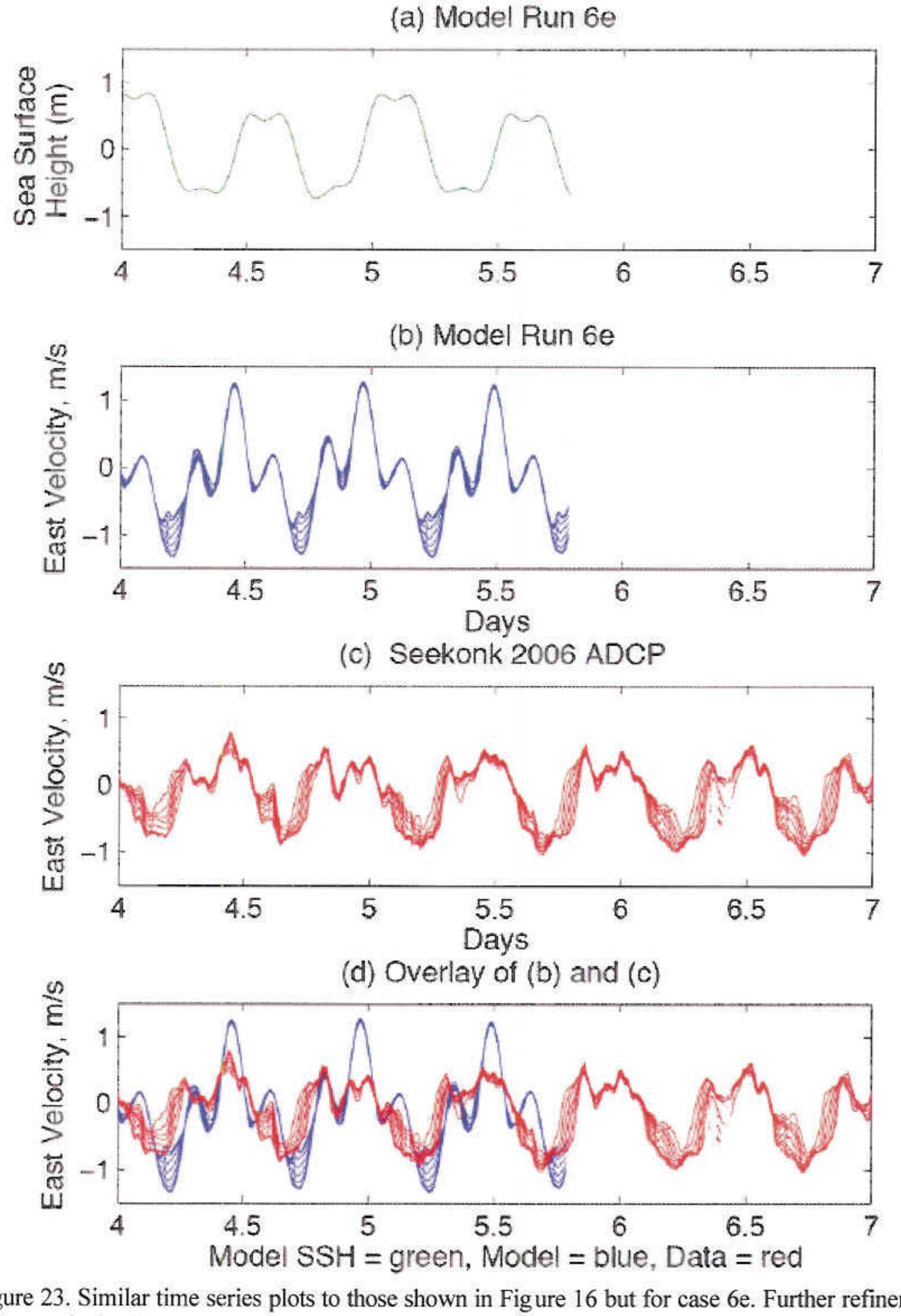

Figure 23. Similar time series plots to those shown in Figure 16 but for case 6e. Further refinements of the numerical grid (Seek1m with a minimum of 1 meter depth on the shoals region of the estuary) lead to very strong mismatch between peak flood and ebb flow rates.

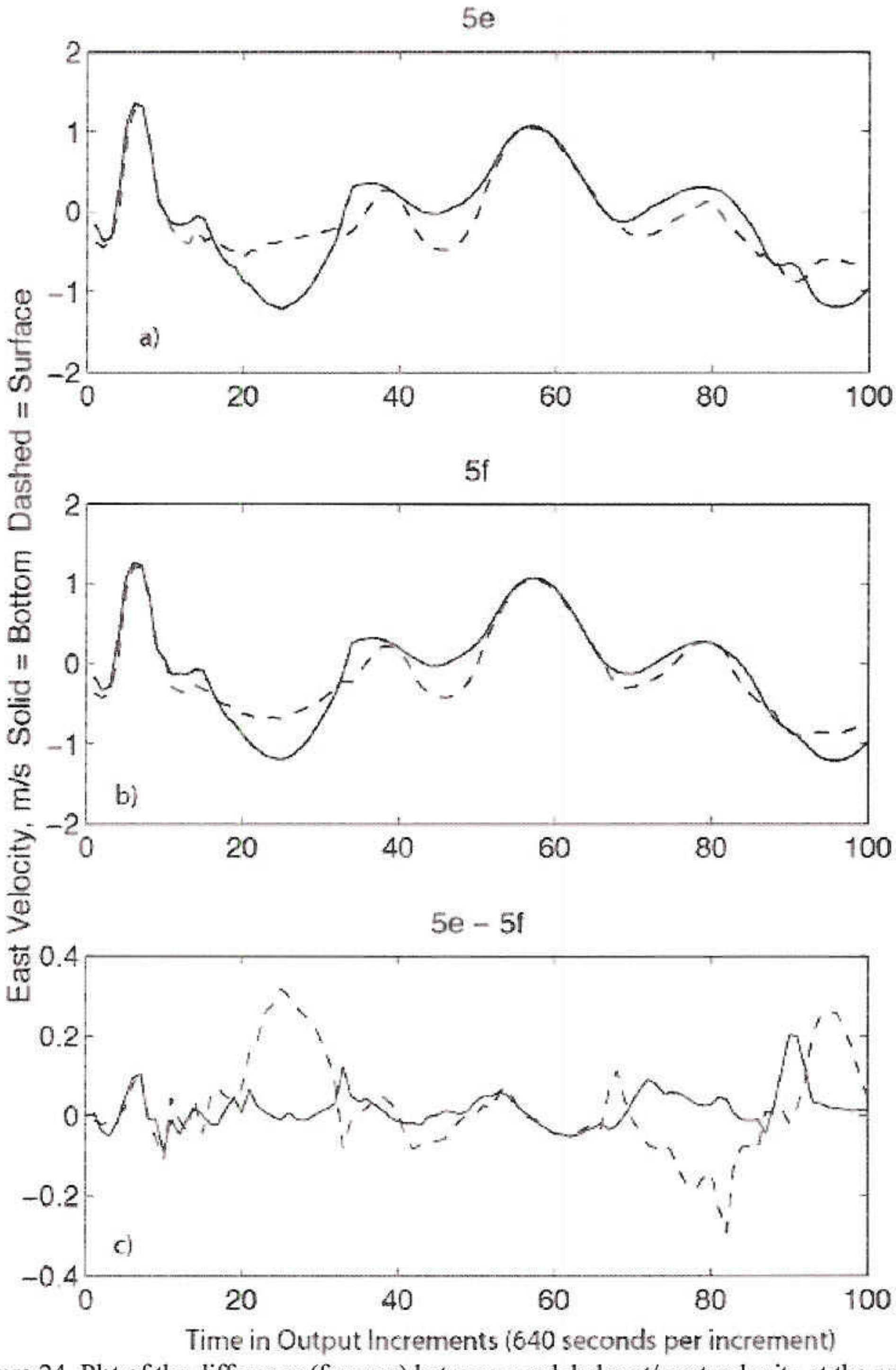

Figure 24. Plot of the difference (frame c) between modeled east/west velocity at the mouth of the Seekonk for cases 5e (frame a) and 5f (frame b) to illustrate the influence of changing Kh parameter. The larger Kh (2 m^2/s versus 1 m^2/s) used in 5f results in larger westward flow of surface water over the duration of the ebb cycle (positive anomaly in c) and a bigger double flood pulse leading into the ebb (negative anomaly in c).

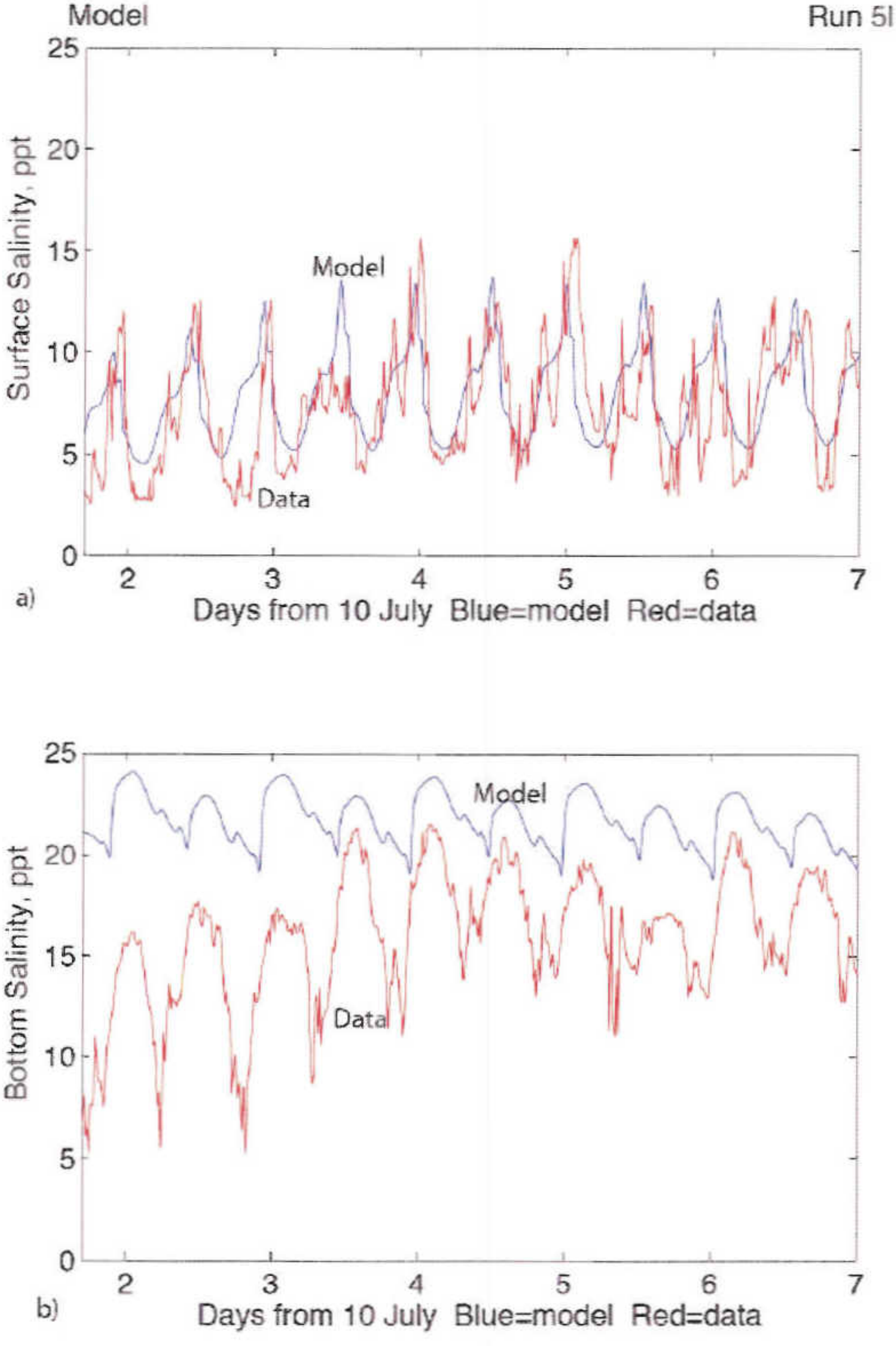

Figure 25. Time series plots of near surface (a) and near bottom (b) salinity (ppt) comparing data from the Phillipsdale station and the model output from this location in the grid. The plots are shown for model run 5l (Table 4). Bottom salinities are too high.

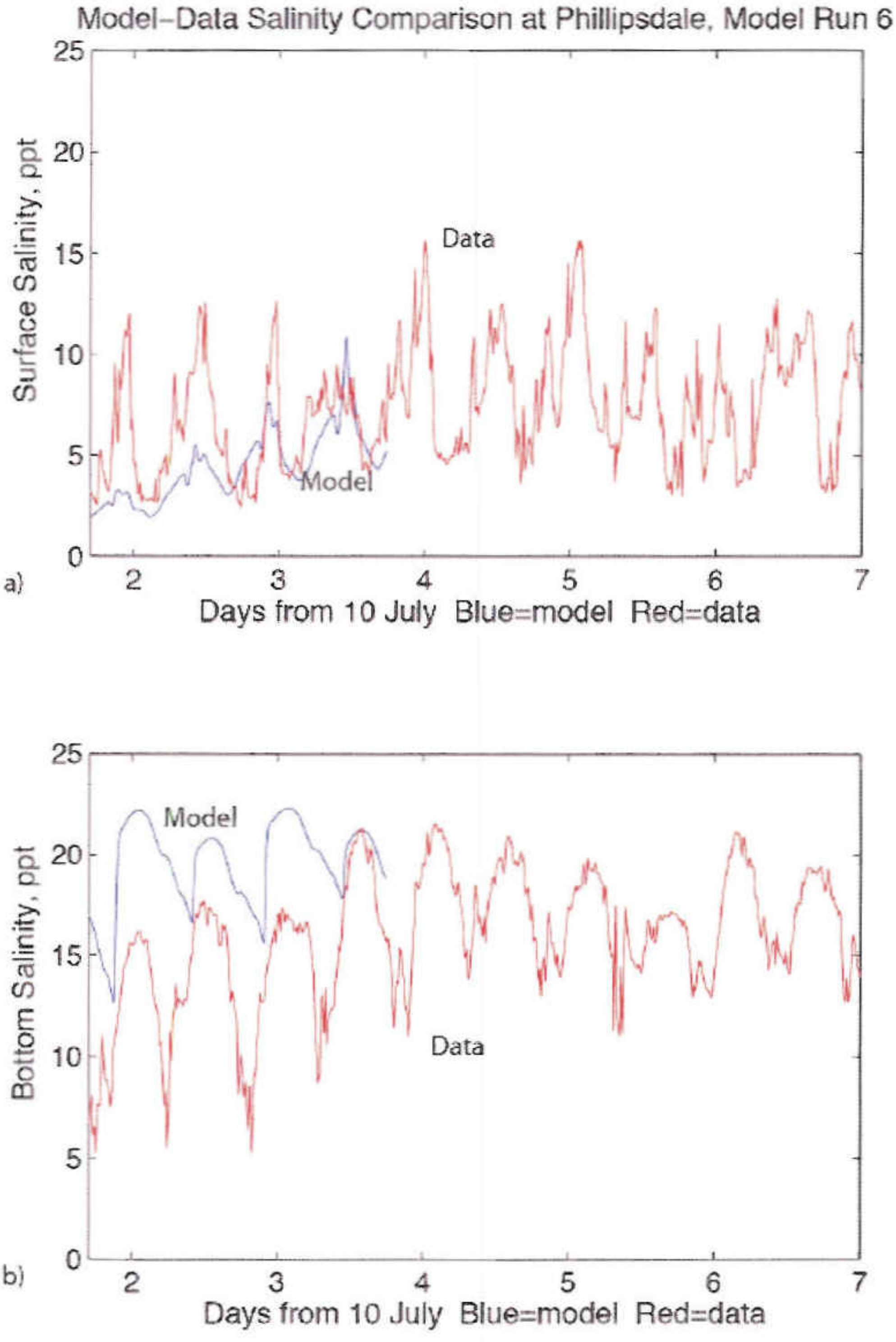

Figure 26. Time series plots of near surface (a) and near bottom (b) salinity (ppt) comparing data from the Phillipsdale station and the model output from this location in the grid. The plots are shown for model run 6b (Table 4). This case uses an improved (Nudging) boundary condition at the southern of the model. Modeled near-bottom salinities are closer to observed values.

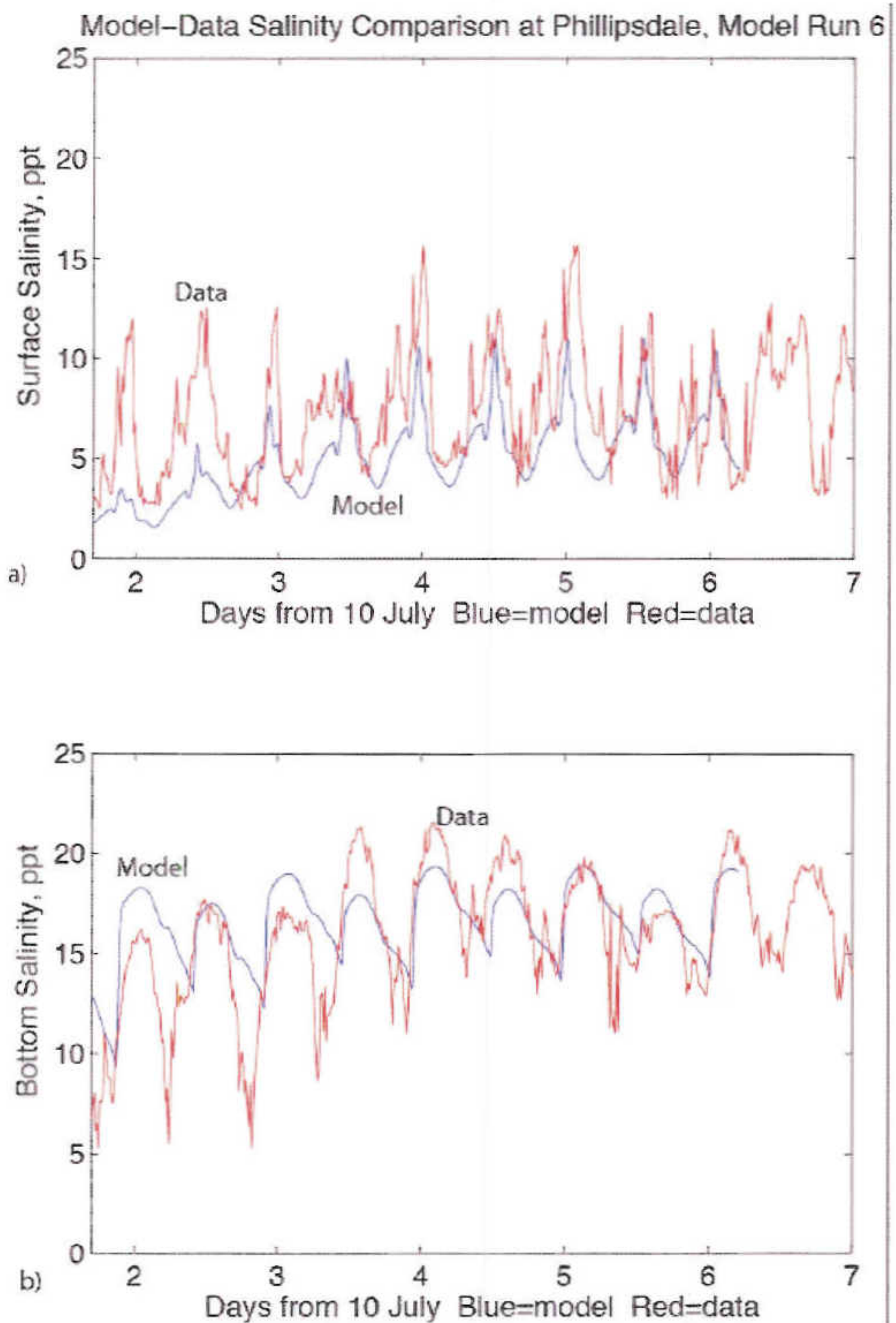

Figure 27. Similar time series data-model comparisons as shown in Figure 26 but for case 6c. Here the change to a clamped southern boundary that forces the southern boundary of the model to maintain a surface to bottom salinity gradient taken from buoy data at the mouth of the Providence River from this period improves the fit for near-bottom records.

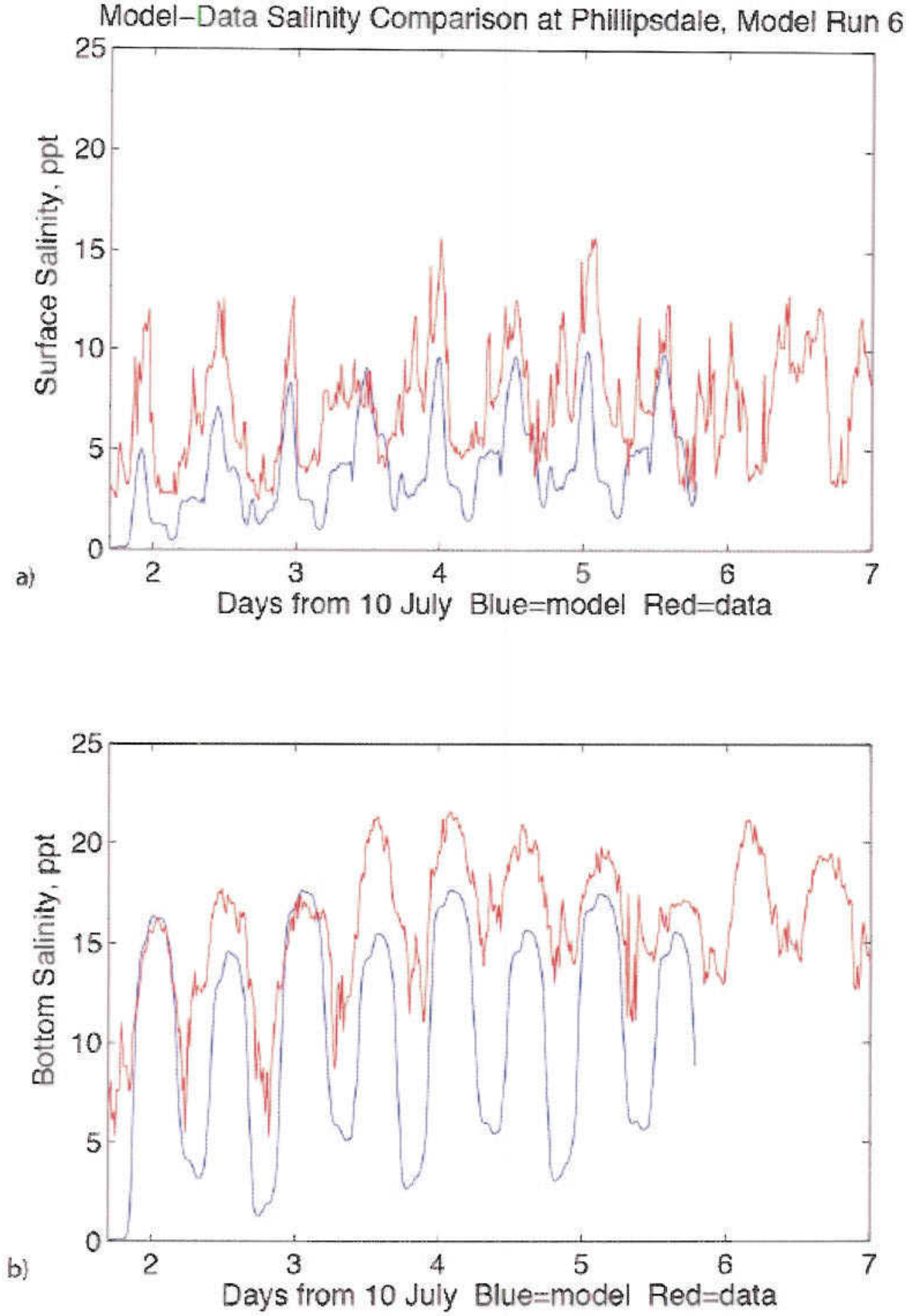

Figure 28. Similar time series plots of observed and modeled salinities as shown in Figure 27 but for case 6f. With the implementation of numerical bathymetry grid that limits the water depth on the shoal regions of the upper estuary to 1m, from 2m, the mean values for near bottom salinity are further reduced.

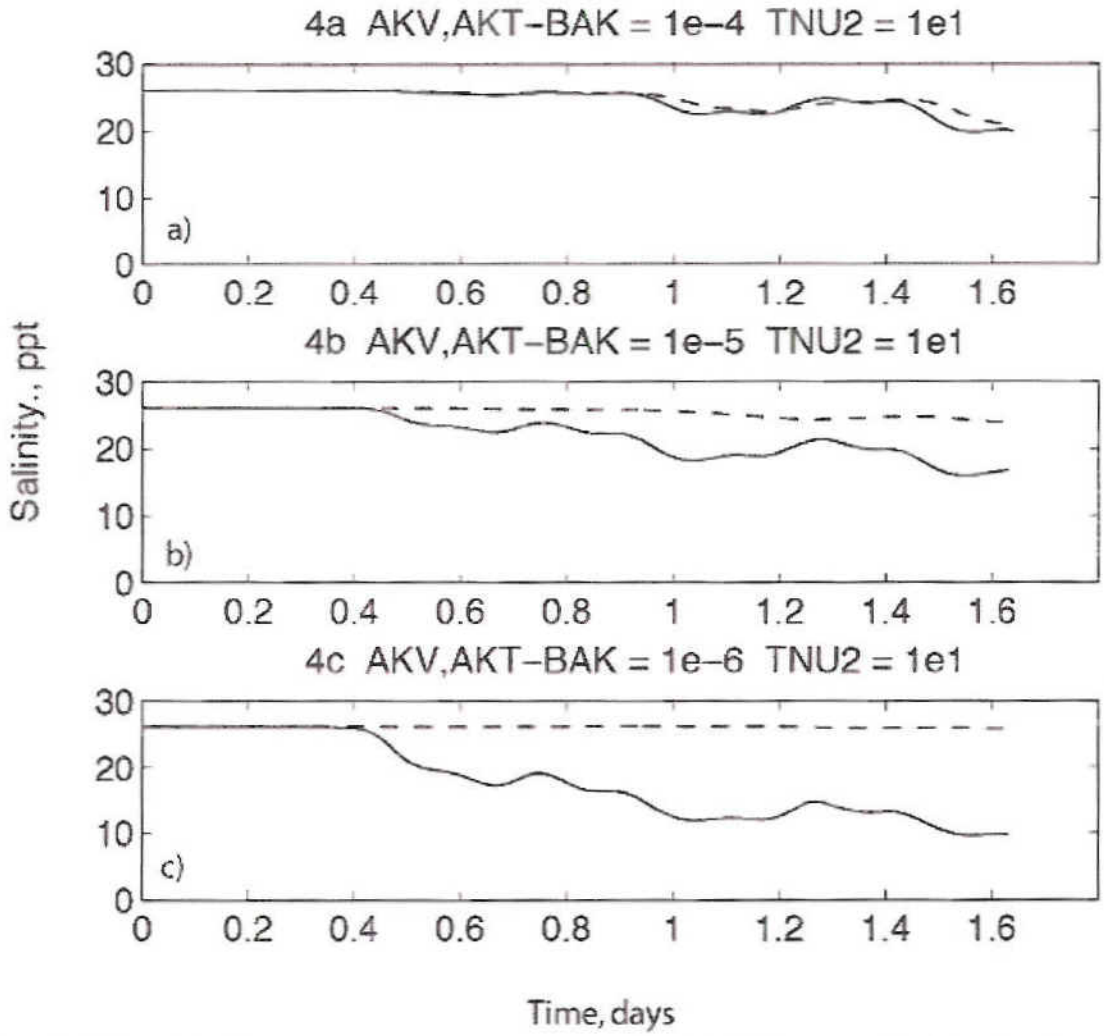

Figure 29. Plots of surface (solid line) and near-bottom (dashed) salinity versus time for a location near the Phillipsdale station. Plots are from cases with constant mixing coefficients (model series runs labeled 4 in Table 4) but with decreasing values for Kv (vertical mixing parameter). Values for Kv change from a) 10^{-4}, b) 10^{-5}, and c) 10^{-6}.